Cell Reports

Article

Salmonella T3SS-2 virulence enhances gut-luminal colonization by enabling chemotaxis-dependent exploitation of intestinal inflammation

Graphical abstract

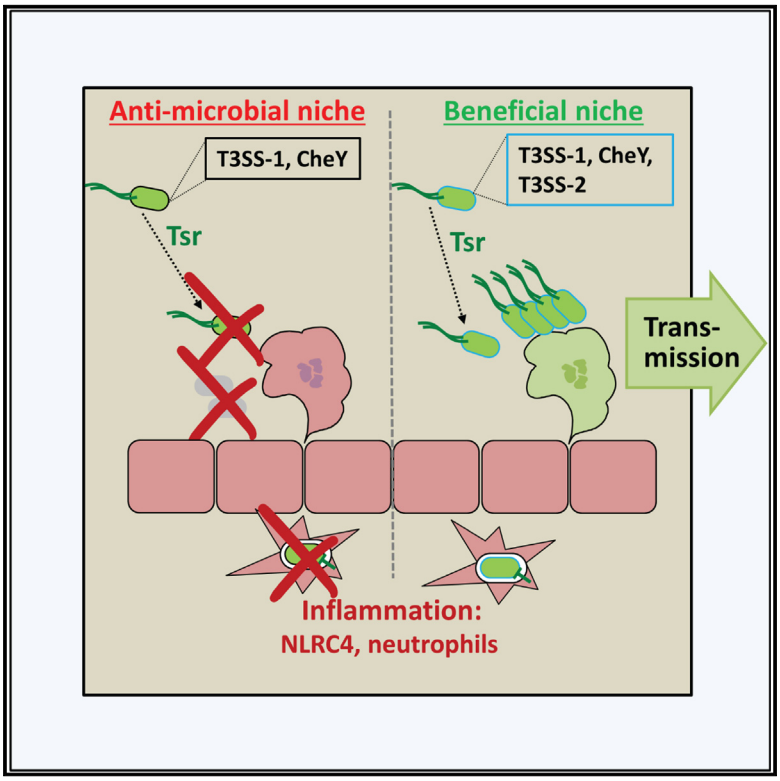

Highlights

- Tsr chemotaxis enables *Salmonella* to exploit nutritional niches near inflamed epithelium
- In *S.*Tm 14028, strain-specific virulence factors impact pathogen's gut colonization
- T3SS-2 virulence is crucial for surviving host's NLRC4 inflammasome and neutrophil effects
- Germ-free mice exhibit a similar inflammatory landscape to antibiotic-pre-treated mice

Authors

Ersin Gül, Jemina Huuskonen, Andrew Abi Younes, ..., Mikael E. Sellin, Erik Bakkeren, Wolf-Dietrich Hardt

Correspondence

ersing@ethz.ch (E.G.), hardt@micro.biol.ethz.ch (W.-D.H.)

In brief

Gül et al. show that *Salmonella*'s exploitation of gut inflammation through chemotaxis hinges on T3SS-2 and strain-specific virulence factors. When *Salmonella* cannot secrete T3SS-2 effectors, the host's NLRC4 inflammasome and neutrophils create a hostile microenvironment for the pathogen.

Gül et al., 2024, Cell Reports *43*, 113925
March 26, 2024
https://doi.org/10.1016/j.celrep.2024.113925

CellPress

Cell Reports

CellPress
OPEN ACCESS

Article

Salmonella T3SS-2 virulence enhances gut-luminal colonization by enabling chemotaxis-dependent exploitation of intestinal inflammation

Ersin Gül,[1,*] Jemina Huuskonen,[1,8] Andrew Abi Younes,[1,8] Luca Maurer,[1] Ursina Enz,[1] Jakob Zimmermann,[2,3] Mikael E. Sellin,[4,5] Erik Bakkeren,[1,6,7] and Wolf-Dietrich Hardt[1,9,*]

[1]Institute of Microbiology, Department of Biology, ETH Zurich, Zurich, Switzerland
[2]Department of Visceral Surgery and Medicine, Inselspital, Bern University Hospital, University of Bern, Bern, Switzerland
[3]Department for Biomedical Research, University of Bern, Bern, Switzerland
[4]Department of Medical Biochemistry and Microbiology, Uppsala University, Uppsala, Sweden
[5]Science for Life Laboratory, Uppsala, Sweden
[6]Present address: Department of Biology, University of Oxford, Oxford, UK
[7]Present address: Department of Biochemistry, University of Oxford, Oxford, UK
[8]These authors contributed equally
[9]Lead contact
*Correspondence: ersing@ethz.ch (E.G.), hardt@micro.biol.ethz.ch (W.-D.H.)
https://doi.org/10.1016/j.celrep.2024.113925

SUMMARY

Salmonella Typhimurium (*S*.Tm) utilizes the chemotaxis receptor Tsr to exploit gut inflammation. However, the characteristics of this exploitation and the mechanism(s) employed by the pathogen to circumvent antimicrobial effects of inflammation are poorly defined. Here, using different naturally occurring *S*.Tm strains (SL1344 and 14028) and competitive infection experiments, we demonstrate that type-three secretion system (T3SS)-2 virulence is indispensable for the beneficial effects of Tsr-directed chemotaxis. The removal of the 14028-specific prophage Gifsy3, encoding virulence effectors, results in the loss of the Tsr-mediated fitness advantage in that strain. Surprisingly, without T3SS-2 effector secretion, chemotaxis toward the gut epithelium using Tsr becomes disadvantageous for either strain. Our findings reveal that luminal neutrophils recruited as a result of NLRC4 inflammasome activation locally counteract *S*.Tm cells exploiting the byproducts of the host immune response. This work highlights a mechanism by which *S*.Tm exploitation of gut inflammation for colonization relies on the coordinated effects of chemotaxis and T3SS activities.

INTRODUCTION

Several enteric pathogens, including *Salmonella enterica* serovar Typhimurium (or *Salmonella* Typhimurium; hereafter *S*.Tm), trigger gut inflammation to modify the gut environment and create an advantageous niche for themselves in the host's intestine.[1–4] Notably, the inflamed gut features both inflammation-dependent nutrients, which can fuel pathogen growth, as well as antimicrobial activities. The pathogen's strategy allows it to efficiently compete with the resident microbiota.[1–4] To engage with the gut tissue and reap the benefits of gut inflammation, pathogens like *S*.Tm utilize receptor-mediated chemotaxis to direct themselves toward microhabitats enriched in nutrients generated as a result of host immune responses.[5,6] However, the most favorable gut-luminal microhabitats are often constructed near the epithelium,[7] which is also where the strongest immune defenses can be found. In response to *S*.Tm tissue invasion, the host NLRC4 inflammasome in epithelial cells initiates a series of responses that result in the expulsion of infected epithelial cells, secretion of immune mediators, recruitment of natural killer cells and neutrophils into the lamina propria, and neutrophil *trans*-migration into the gut lumen.[8–13] These strong immune responses can block pathogen access to the gut epithelium and kill nearby pathogen cells.[12–14] It is still not well understood how *S*.Tm can benefit from the consequences of gut inflammation without suffering too greatly from its antimicrobial effects.

S.Tm utilizes its type-three secretion systems (T3SS) 1 and 2 (encoded on *Salmonella* pathogenicity islands [SPI] 1 and 2, respectively) to invade the intestinal epithelium, trigger gut inflammation, colonize the deeper gut tissue, and further enhance enteropathy.[15] *S*.Tm can secrete diverse cocktails of effectors into host cells using both T3SS-1 and -2 to manipulate host cell physiology.[16–18] Many SPI-1 effectors injected by T3SS-1 facilitate the invasion of epithelial cells,[17] while SPI-2 effectors injected by T3SS-2 are generally thought to promote growth and survival of the pathogen in the host's tissue (i.e., lamina propria, where myeloid cells often reside).[18–22] In some cases, effectors for either T3SS-1 or T3SS-2 can be encoded on prophages. The acquisition of phage-carried virulence factors is often strain specific and contributes to the high diversity between different *S*.Tm strains.[23–25] For example, genes encoding for different *S*.Tm E3 ubiquitin ligases (e.g., SlrP or SspH1) that

are used by the pathogen to manipulate the host physiology during invasion were shown to be differentially present across *S*.Tm strains.[26–30] Even though direct experimental evidence is lacking for most cases, it is thought that the horizontal acquisition of these factors contributes to the host range of different *S*.Tm strains.

The *S*.Tm chemotaxis receptor Tsr is one of the best-characterized receptors, and it is involved in chemotaxis toward host-derived nitrate (also termed "energy taxis"),[6,31] which is elevated during gut inflammation.[7,32] Notably, the Tsr receptor is also implicated in *E. coli* chemotaxis toward nitrate in the inflamed gut.[7,33] Previous work using *S*.Tm ATCC14028 and a murine typhoid model showed that Tsr-mediated energy taxis in the ileum is dependent on the constitutive basal expression of Nos2 in epithelial cells and phagocytes in this region.[31] Similar studies in antibiotic-pre-treated mouse models identified that *S*.Tm Tsr is crucial for pathogen cells to reach the epithelium and initiate systemic infections.[6,7] Competitive infection experiments revealed that the *tsr* mutants grow less efficiently than wild-type (WT) counterparts and that Tsr-mediated chemotaxis toward the gut epithelium is an important strategy for *S*.Tm strain ATCC14028 to flourish during inflammation.[6,7] Strikingly, however, experimental evolution studies at the same time showed that *Salmonella* populations (of strain SL1344) in the gut accumulate loss-of-function mutations in several genes, including *tsr*.[34,35] Similarly, *tsr* mutations appear to be selected for in some natural endemic *S*.Tm strains.[36] Moreover, recent bioinformatics analysis of more than 100,000 *Salmonella* genomes identified the *tsr* locus as one of the most frequently mutated genetic regions in natural isolates.[37] The high prevalence of *tsr* mutations suggests that some poorly defined niches select for *tsr* mutants. However, no direct evidence has been presented so far.

Overall, these findings from experimental evolution[34,35] and genome-based studies[36,37] seem at odds with the well-established beneficial role[6,7] of Tsr-mediated chemotaxis during gut inflammation. Therefore, it remains unclear which circumstances select for WT or mutant *tsr* alleles. Here, we applied a systematic approach to address this open question using different *S*.Tm strains and competitive infection experiments in a series of immune-proficient and -deficient mouse models.

RESULTS

In *S*.Tm 14028, the fitness benefit associated with *tsr* in the inflamed gut depends on the virulence factors encoded by the prophage Gifsy3

Previous studies assessing the selection for or against *tsr*-disrupting mutations were performed in different *Salmonella* strains. While experiments in which *tsr* conferred a fitness advantage[6,7,31] were conducted using the common strain *S*.Tm ATCC14028 (isolated from chicken[38]; denoted here as 14028), experimental evolution work[34] employed another common strain, *S*.Tm SL1344 (a laboratory-derived strain generated by introducing a histidine auxotrophy into the strain *S*.Tm 4/74, which had been isolated from cattle[39,40]; denoted here as SL1344). To investigate if genomic differences between these two strains could explain the fitness advantage or disadvantage associated with the Tsr chemotaxis receptor, we performed infection experiments using 14028 and SL1344. We created isogenic *tsr*-deficient mutants for each strain (14028 *Δtsr* and SL1344 *Δtsr*, respectively). To test the fitness of these mutants against their WT counterparts, we performed competitive infections in the well-established streptomycin-pre-treated mouse model.[41] We orally infected streptomycin-pre-treated C57BL/6 mice with a 1:1 mixture of *tsr*-deficient and *tsr*-proficient 14028 (14028 *Δtsr* vs. 14028 WT) or SL1344 (SL1344 *Δtsr* vs. SL1344 WT) for 3 or 4 days (5×10^7 colony-forming units [CFUs] in total, by gavage; experimental scheme in Figure 1A). In the 14028 background, *tsr*-deficient *Salmonella* cells showed attenuated gut-luminal colonization compared to the WT starting from day 2 post-infection (p.i.) (competitive index [C.I.] < 0.01 at day 4 p.i.; Figures 1B and S1A) as reported before.[7] In contrast, the *tsr* mutant of SL1344 featured WT levels of gut-luminal growth during the entire course of the infection (Figures 1B and S1A). Similarly, we observed an attenuation of *tsr*-deficient 14028 in the mesenteric lymph node (mLN), while SL1344 *Δtsr* colonized the mLN equally well as the isogenic WT strain (Figures 1C and S1B). Comparable levels of gut inflammation (assessed by the general marker Lipocalin-2[42] in feces) were observed in both strain backgrounds, suggesting that other factors might be responsible for the observed differences between the two strains (Figure 1D).

Next, we aimed to determine why *tsr* mutations attenuate 14028 but not SL1344. We compared the genomes of these two strains, focusing on prophages, as they often contribute to *S*.Tm strain diversity.[23,36] Gifsy3 is an interesting candidate, as this phage is present in 14028, but not in SL1344, and contains a gene for a T3SS effector protein implicated in virulence[26,27,43–45] (Figure 1E). To test if the differential presence of the prophage Gifsy3 enables a fitness advantage to *tsr*-proficient cells in the 14028 background, we created a deletion mutant lacking the entire prophage (denoted as 14028 Δ*Gifsy3*) and a *tsr*-deficient counterpart of this strain (14028 Δ*Gifsy3*Δ*tsr*). We repeated the competitive infection experiment as in Figure 1B with these two strains (14028 Δ*Gifsy3*Δ*tsr* vs. 14028 Δ*Gifsy3*). In this experiment, we limited the infection to 3 days, as 3 days sufficed to observe Tsr-linked fitness benefits in 14028 (Figure 1B). Strikingly, in the absence of Gifsy3, the *tsr* mutant colonized the gut lumen (ca. 10^9 CFU/g feces; at the carrying capacity) equally well as the isogenic *tsr*-proficient strain (C.I. ≈ 1 for 14028 Δ*Gifsy3*Δ*tsr* vs. 14028 Δ*Gifsy3*; Figures 1F and S1C). This was in stark contrast to the pronounced attenuation of the *tsr*-deficient cells in the WT 14028 background (14028 WT; data combined from Figure 1 days 1–3 and the new experiment; C.I. < 0.05 at day 3 p.i.; Figures 1F and S1C). Furthermore, in the 14028 Δ*Gifsy3* background, the *tsr*-proficient strain colonized the mLN or the cecal tissue equally well as the *tsr* mutant (Figures 1G and S1D–S1F). Altogether, these data suggest that the fitness advantage associated with Tsr in 14028 is strongly dependent on the prophage Gifsy3.

Then, we asked if some virulence factor(s) encoded on Gifsy3 could enable the fitness advantage reaped via Tsr. Previous work already revealed that one of the effector proteins encoded on Gifsy3, SspH1, is involved in *Salmonella* virulence.[27,28,30,46,47] Therefore, we created *tsr*-deficient and -proficient strain pairs in a 14028 background lacking *sspH1* (14028 Δ*sspH1*Δ*tsr* vs.

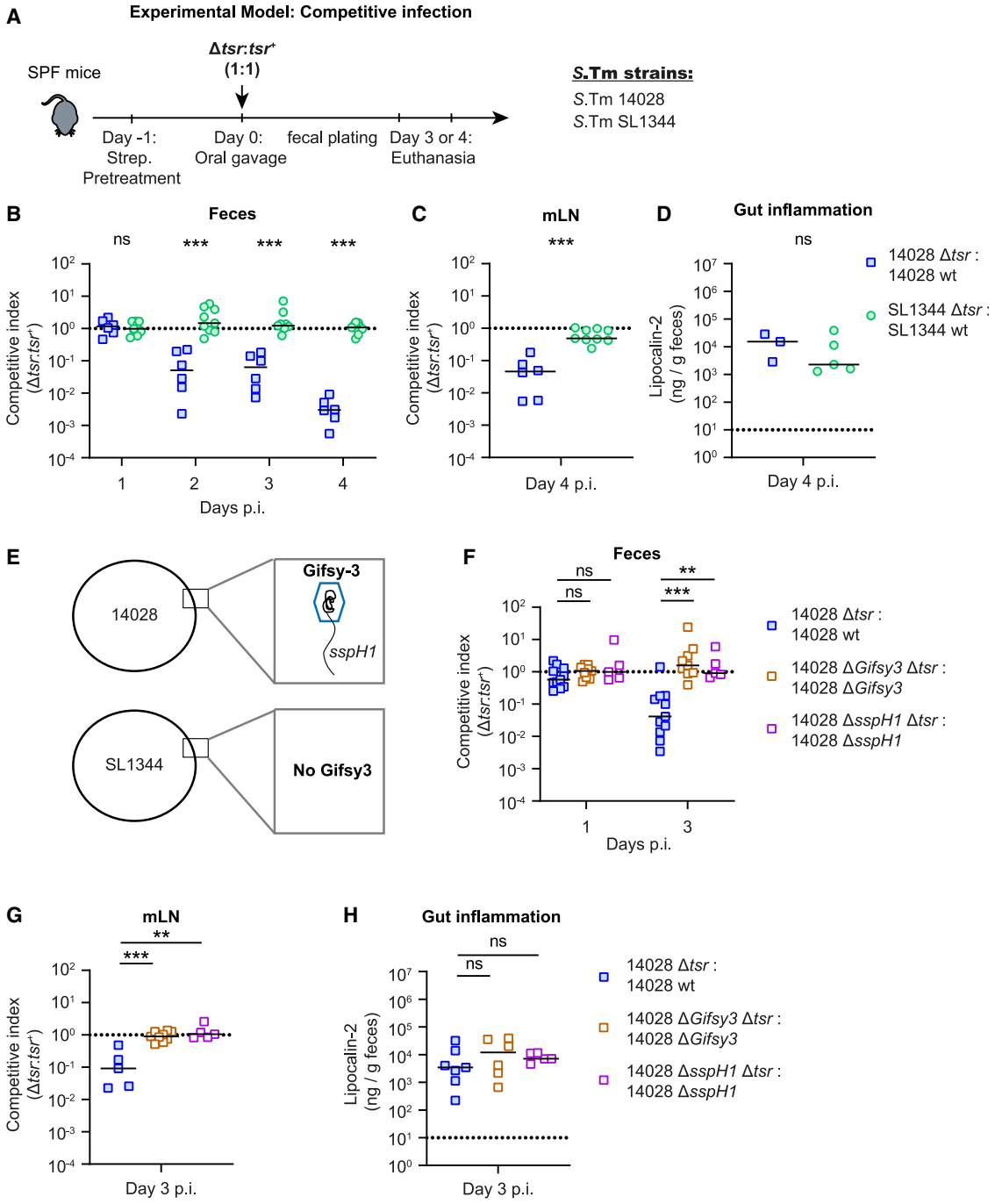

Figure 1. Dependency of the Tsr-mediated fitness advantage on the strain background of *S*.Tm

(A) Experimental approach.

(B–D) Streptomycin-pre-treated C57BL/6 mice infected orally with a 1:1 mixture of 14028 Δ*tsr:*14028 WT (blue squares) or SL1344 Δ*tsr*:SL1344 WT (green circles) for 4 days (5×10^7 CFUs total). The C.I. calculated as the ratio of *tsr* deficient/*tsr* proficient, determined by selective plating, normalized to the inoculum.

(B and C) The C.I.s (B) in feces and (C) in mLN.

(D) Fecal Lipocalin-2 concentrations as a measure of gut inflammation. Dotted line: detection limit.

(E) Representation of the differentially present prophages in both strains.

(F and G) Three day competitive infection with 14028 Δ*tsr*:14028 WT (1:1; blue squares; combined data from B and C), 14028 Δ*Gifsy3*Δ*tsr*:14028 Δ*Gifsy3* (1:1; brown squares), or 14028 Δ*sspH1*Δ*tsr*:14028 Δ*sspH1* (1:1; purple squares). The C.I.s (F) in feces and (G) in mLN. Lines: median. Dotted lines: C.I. of 1.

(H) Fecal Lipocalin-2 concentrations. Dotted line: detection limit.

(legend continued on next page)

14028 Δ*sspH1*) and performed competitive infections as described in Figures 1A and 1B. Similar to the 14028 Δ*Gifsy3* background, the attenuation associated with Tsr deficiency was absent in the 14028 Δ*sspH1* background (Figures 1E, 1F, and S1C–S1E). Both strains reached equally high pathogen densities in the feces at day 1 p.i. and were also recovered at equal densities in the feces at day 3 p.i. (C.I. ≈1; Figures 1F and S1C). Similarly, 14028 Δ*sspH1*Δ*tsr* colonized the mLN and the cecal tissue equally well as 14028 Δ*sspH1* (Figures 1G and S1D–S1E). Therefore, the *sspH1* deletion phenocopies the deletion of the entire *Gifsy3* prophage region. Notably, the deletion of *Gifsy3* or *sspH1* did not influence the general ability of these strains to trigger gut inflammation, as Lipocalin-2 levels were comparable to 14028 WT background (Figure 1H).

Taken together, our results demonstrate that in the inflamed gut, the Tsr chemotaxis receptor confers a fitness advantage only in the strain background of 14028 and that this advantage is dependent on the virulence factors encoded by the prophage Gifsy3. While this explains a strain-specific fitness advantage of Tsr chemotaxis, it still does not explain why the loss of Tsr seems to be beneficial in some cases.

Tsr-mediated chemotaxis is detrimental for *S.*Tm if the pathogen cannot secrete T3SS-2 effectors

We thus set out to investigate the characteristics of selection for *tsr* mutants observed in a percentage of natural isolates[36,37] and experimental evolution work.[34,35] As shown in Figure 1, while the beneficial role of *tsr* was abolished in 14028 Δ*Gifsy3* and not detectable in SL1344 (naturally lacking *Gifsy3*) (i.e., C.I. ≈1), we did not observe a selection for *tsr* mutants (i.e., mutant vs. WT C.I. > 1). This suggested that additional factors, not picked up by our current setup, are at play, leading to counterselection against *tsr*. Notably, the previous experiments highlighting the loss-of-function mutations in *tsr* were conducted using a mutant SL1344 strain that lacks the ability to secrete virulence effectors via T3SS-2 (i.e., SL1344 Δ*ssaV*; gene encoding a structural component of the needle protein).[34] Thus, we hypothesized that T3SS-2 virulence might be necessary to support pathogen survival in the niche, to which *S.*Tm is guided by Tsr chemotaxis. To test this, we constructed *tsr*-proficient and -deficient strains in the SL1344 background lacking the T3SS-2 apparatus and performed competitive infections for 4 days in antibiotic-pre-treated mice (SL1344 Δ*ssaV*Δ*tsr* vs. SL1344 Δ*ssaV*; Figures 2A–2C, empty black circles). We compared these results to the WT SL1344 background (SL1344 WT; re-plotted from Figure 1, filled green circles). Indeed, *tsr*-proficient cells were strongly selected against in mice infected with SL1344 Δ*ssaV*, while *tsr*-deficient and -proficient cells had equal densities in the feces of mice infected with SL1344 WT (Figures 2A and S2A; C.I. ≈300 vs. ≈1 at day 4 p.i., respectively). Similar results were observed in the mLNs of these mice (Figures 2B and S2B). Of note, mice infected with the SL1344 Δ*ssaV* strain mixture also showed signs of robust gut inflammation (i.e., [Lipocalin-2] > 1,000 ng/g feces), suggesting that the selection occurs in the inflamed gut (Figure 2C). Thus, we conclude that selection for *tsr* mutants observed in the SL1344 background[34] is linked to a non-functional T3SS-2.

We asked if the beneficial effects of Tsr chemotaxis (only observed in 14028 WT background) could be the combined effect of T3SS-2 virulence and the effectors encoded on Gifsy3. We reasoned that if the fitness advantage of *tsr*-proficient cells is abolished in the 14028 Δ*ssaV* background, then this would suggest that T3SS-2 functionality has a general role in enabling chemotaxis-dependent pathogen survival or growth in the inflamed gut. To test this, we created additional mutants in a 14028 background lacking the ability to secrete effectors through T3SS-2, and we performed competitive infection experiments in antibiotic-pre-treated mice for 4 days (14028 Δ*ssaV*Δ*tsr* vs. 14028 Δ*ssaV*). We compared C.I.s to those obtained in the 14028 WT background (re-plotted from Figures 1B and 1C for reference, filled blue squares). When the T3SS-2 needle was non-functional (i.e., 14028 Δ*ssaV*), the *tsr*-proficient strain no longer had a fitness advantage over the *tsr*-deficient mutant strain (Figure 2D). Strikingly, opposite to the competitive advantage in the 14028 WT background, *tsr*-proficient cells were outcompeted by *tsr*-deficient cells in the 14028 Δ*ssaV* background (Figures 2D and S2A). In fact, losing the ability to secrete effectors through T3SS-2 had a >10,000-fold effect on the gut colonization of *tsr*-proficient cells compared to the isogenic *tsr*-deficient counterparts during acute gut infection (C.I. of *tsr*-deficient/*tsr*-proficient cells <0.01 in WT 14028 vs. >90 in 14028 Δ*ssaV* background). Furthermore, *tsr*-proficient cells colonized the mLNs less efficiently in 14028 Δ*ssaV* background than they did in the 14028 WT background (C.I. > 3 vs. C.I. < 0.01; Figures 2E and S2B). Notably, the competitive advantage of *tsr*-deficient cells over *tsr*-proficient cells in 14028 Δ*ssaV* background was comparable to the one in the SL1344 Δ*ssaV* background (compare empty black squares from Figure 2D to empty black circles from Figure 2A; C.I. ≈330 vs. ≈100 at day 4 p.i.). Similarly, mice infected with the 14028 Δ*ssaV* strain mixture also still showed signs of robust gut inflammation (Figure 2F; [Lipocalin-2] > 1,000 ng/g feces). To assess how Tsr affects fitness beyond day 4 and if this is dependent on the T3SS-2 apparatus, we utilized another mouse model. We performed competitive infections in streptomycin-pre-treated 129SvEv mice, which can survive the orogastric infection for longer periods thanks to a functional Nramp1 protein,[48] and checked Tsr fitness in the background of 14028 and 14028 Δ*ssaV* for 14 days. The day 7 data indicated that Tsr affects 14028 fitness beyond day 4 (Figure S2C). However, we cannot confidently interpret the phenotypes beyond day 7, as natural mutants in *hilD* (and other genes) are known to be selected and dominate the luminal *Salmonella* population, thus modifying its capacity to sustain gut inflammation by day 10 p.i. in that model.[34,35] Anyhow, while the *tsr*$^+$ cells continued to show a fitness advantage (up to 10,000-fold) in 14028 WT infected mice, they continued to suffer from reduced fitness in 14028 Δ*ssaV* infected mice (Figure S2C).

(B and C) 4 independent experiments; 2 for each group; 14028 (n = 6 mice) and SL1344 (n = 9 mice). (F and G) 6 independent experiments; 4 for 14028, 2 for 14028 Δ*Gifsy3*, and 1 for 14028 Δ*sspH1* (2 different cohorts). 14028 (n = 11 mice), 14028 Δ*Gifsy3* (n = 9 mice), and 14028 Δ*sspH1* (n = 5 mice). Two-tailed Mann Whitney U tests to compare two groups in each image. Not significant (ns) $p \geq 0.05$, $^{**}p < 0.01$, and $^{***}p < 0.001$.

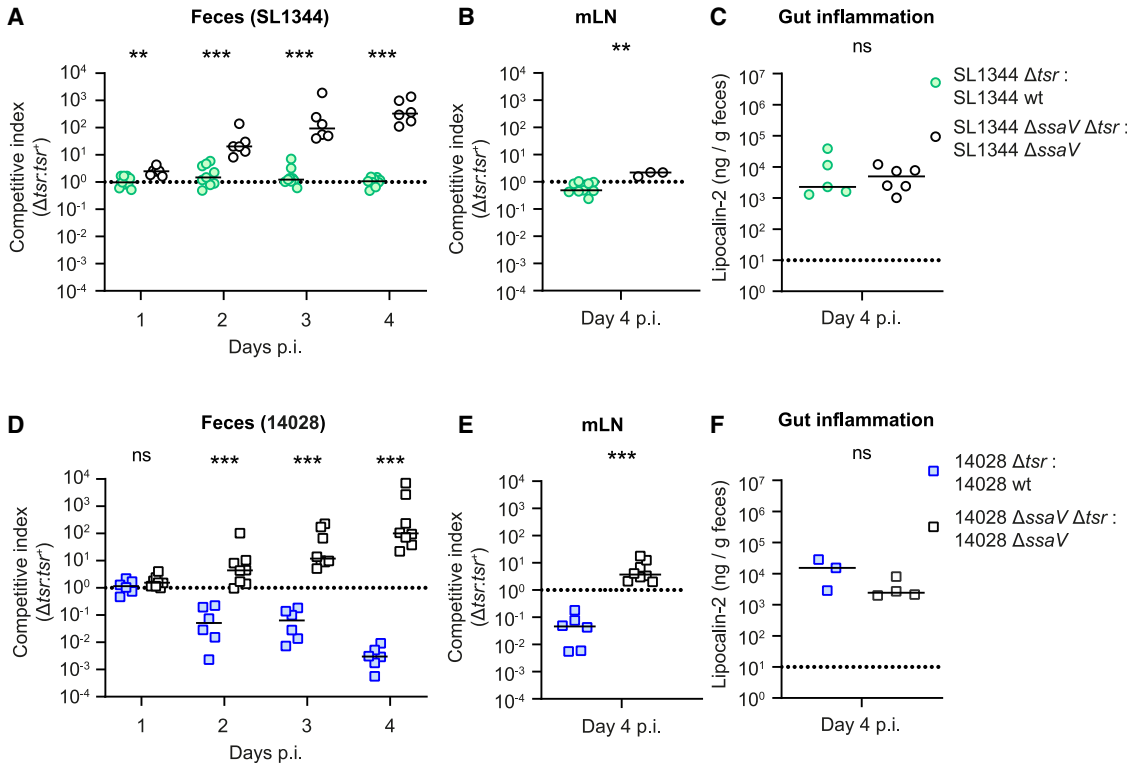

Figure 2. Effect of T3SS-2 deficiency on the fitness advantage associated with Tsr

Competitive infections in streptomycin- or ampicillin-pre-treated C57BL/6 mice with SL1344 Δ*ssaV*Δ*tsr*:SL1344 Δ*ssaV* (empty black circles; compared to data from Figure 1B) or 14028 Δ*ssaV*Δ*tsr*:14028 Δ*ssaV* (empty black squares; compared to data from Figure 1B). The C.I.s (A and D) in feces and (B and E) in mLN for indicated strain combinations. Lines: median. Dotted lines: C.I. of 1. (C and F) Fecal Lipocalin-2 concentrations. Dotted line: detection limit. (A) 4 independent experiments; 2 for SL1344 (n = 9 mice; from Figure 1B), 2 for SL1344 Δ*ssaV* (n = 6; 3 mice streptomycin pre-treated, 3 mice ampicillin pre-treated; results were indistinguishable between treatments). (D) 5 independent experiments; 2 for 14028 (n = 6 mice; from Figure 1B), 3 for 14028 Δ*ssaV* (n = 8; 2 mice streptomycin pre-treated, 6 mice ampicillin pre-treated; results were indistinguishable between treatments). Two-tailed Mann Whitney U tests to compare two groups in each image. ns $p \geq 0.05$, $^{**}p < 0.01$, and $^{***}p < 0.001$.

Collectively, our findings suggest that T3SS-2 virulence is essential for *S*.Tm to survive in the niche to which they are guided by Tsr chemotaxis. This colonization advantage appears to hinge on strain-specific virulence effector(s).

T3SS-2 virulence is required to alleviate the antimicrobial effect of gut inflammation on chemotaxing pathogen cells

Previously, it was shown that *S*.Tm gut-tissue invasion activates the NLRC4 inflammasome in intestinal epithelial cells and that this results in expulsion of the infected cells and recruitment of neutrophils into the gut tissue and the gut lumen.[8–11,49,50] This immune response results in the death of host cells and the release of reactive oxygen and nitrate species, all of which can serve the pathogen as carbon sources or terminal electron acceptors.[6,32] However, such induced immune responses could also be detrimental to the pathogen cells.[12–14] This raises the question of how *Salmonella* can benefit from gut inflammation while also avoiding the potentially detrimental effects of the host immune response. Based on our previous results, we hypothesized that T3SS-2 virulence is essential for the gut-luminal pathogen population to block the antimicrobial effects of host immune cells, which would otherwise kill *tsr*-proficient cells undergoing chemotaxis into desirable niche(s).

To test this hypothesis, we performed series of follow-up experiments in the SL1344 strain background. We chose to continue with this strain background because we already had access to a large collection of site-directed mutants. Moreover, our results from Figure 2 showed that when the T3SS-2 apparatus is non-functional, both strains behave similarly in terms of Tsr-mediated chemotaxis during acute *Salmonella* infection in mice. To this end, we altered the experimental setup slightly and infected the antibiotic-pre-treated mice with an inoculum mixture consisting of three strains instead of two. We added the first strain in excess (SL1344 Δ*ssaV*; 20-fold higher abundance; total of 5×10^7 CFUs; experimental scheme in Figure 3A) as a "conditioning" strain, which is capable of invading tissue and inducing an inflammatory response, while we competed *tsr*-deficient and -proficient cells in a 1:1 ratio in the relevant backgrounds. We used SL1344 Δ*invG*Δ*ssaV* (avirulent; this mutant can perform receptor-mediated chemotaxis but cannot efficiently trigger gut-tissue invasion or inflammation due to lack of SPI-1- and SPI-2-dependent virulence[15]) or SL1344 Δ*ssaV*Δ*cheY* (this mutant cannot perform receptor-mediated

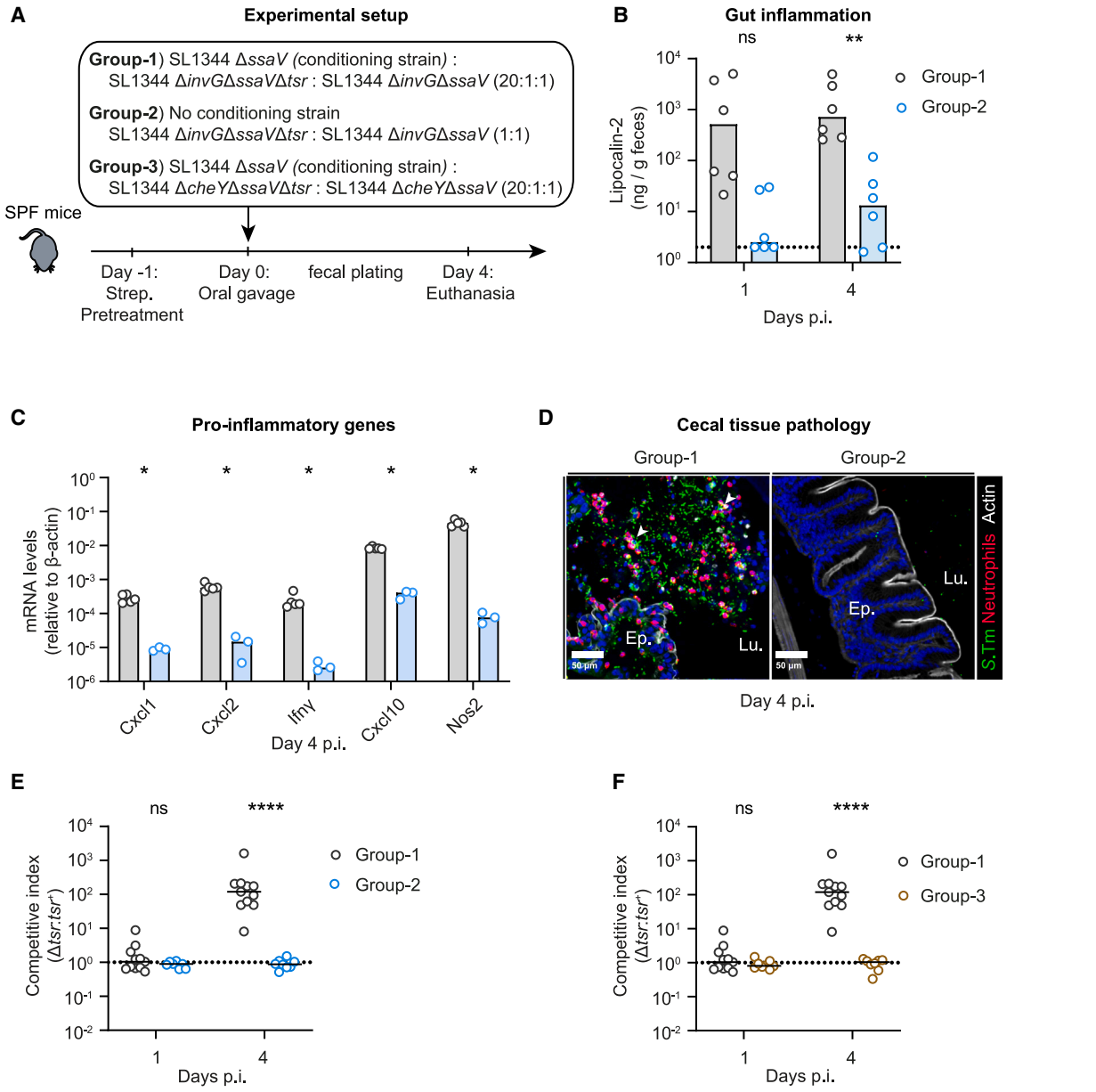

Figure 3. Characterization of the fitness defect associated with Tsr expression in SL1344 Δ*ssaV* background

(A) Experimental setup in (B)–(F). Competitive infection in streptomycin-pre-treated C57BL/6 with group 1: SL1344 Δ*ssaV*:SL1344 Δ*invG*Δ*ssaV*Δ*tsr*:SL1344 Δ*invG*Δ*ssaV* (20:1:1; empty black circles); group 2: SL1344 Δ*invG*Δ*ssaV*Δ*tsr*:SL1344 Δ*invG*Δ*ssaV* (1:1; empty blue circles); and group 3: SL1344 Δ*ssaV*:SL1344 Δ*ssaV*Δ*cheY*Δ*tsr*:SL1344 Δ*ssaV*Δ*cheY* (20:1:1; empty brown circles); in each group, a total 5 × 10^7 CFUs. The C.I. is calculated between the two minor strains and normalized to the inoculum.

(B) Fecal Lipocalin-2 concentrations. Dotted line: detection limit.

(C) Quantification of mRNA expression levels in the cecal mucosa by RT-qPCR. Results are presented relative to β-actin mRNA levels.

(D) Representative micrographs of cecal tissue sections at day 4 p.i., stained for neutrophil marker Ly6B.2 and *Salmonella* lipopolysaccharide (LPS). Blue color: nuclei staining. Lu., lumen; Ep., epithelium. White arrows: *S.*Tm associated with neutrophils in the lumen. Scale bar: 50 μm.

(E and F) The C.I. in feces (group 1 re-plotted). 9 independent experiments; 3 for each group; group 1 (n = 11 mice), group 2 (n = 8 mice), and group 3 (n = 8 mice). Two-tailed Mann Whitney U tests to compare two groups. ns $p \geq 0.05$, *$p < 0.05$, **$p < 0.01$, and ****$p < 0.0001$.

chemotaxis[5]) background strains. In total, we had three groups: the group 1 inoculum consisted of SL1344 Δ*ssaV* (conditioning strain), SL1344 Δ*invG*Δ*ssaV*Δ*tsr*, and SL1344 Δ*invG*Δ*ssaV* (20:1:1, respectively); the group 2 inoculum consisted of SL1344 Δ*invG*Δ*ssaV*Δ*tsr* and SL1344 Δ*invG*Δ*ssaV* (1:1, respectively); and the group 3 inoculum consisted of SL1344 Δ*ssaV,* SL1344 Δ*cheY*Δ*ssaV*Δ*tsr*, and SL1344 Δ*cheY*Δ*ssaV* (20:1:1, respectively). This approach ensured that the additional

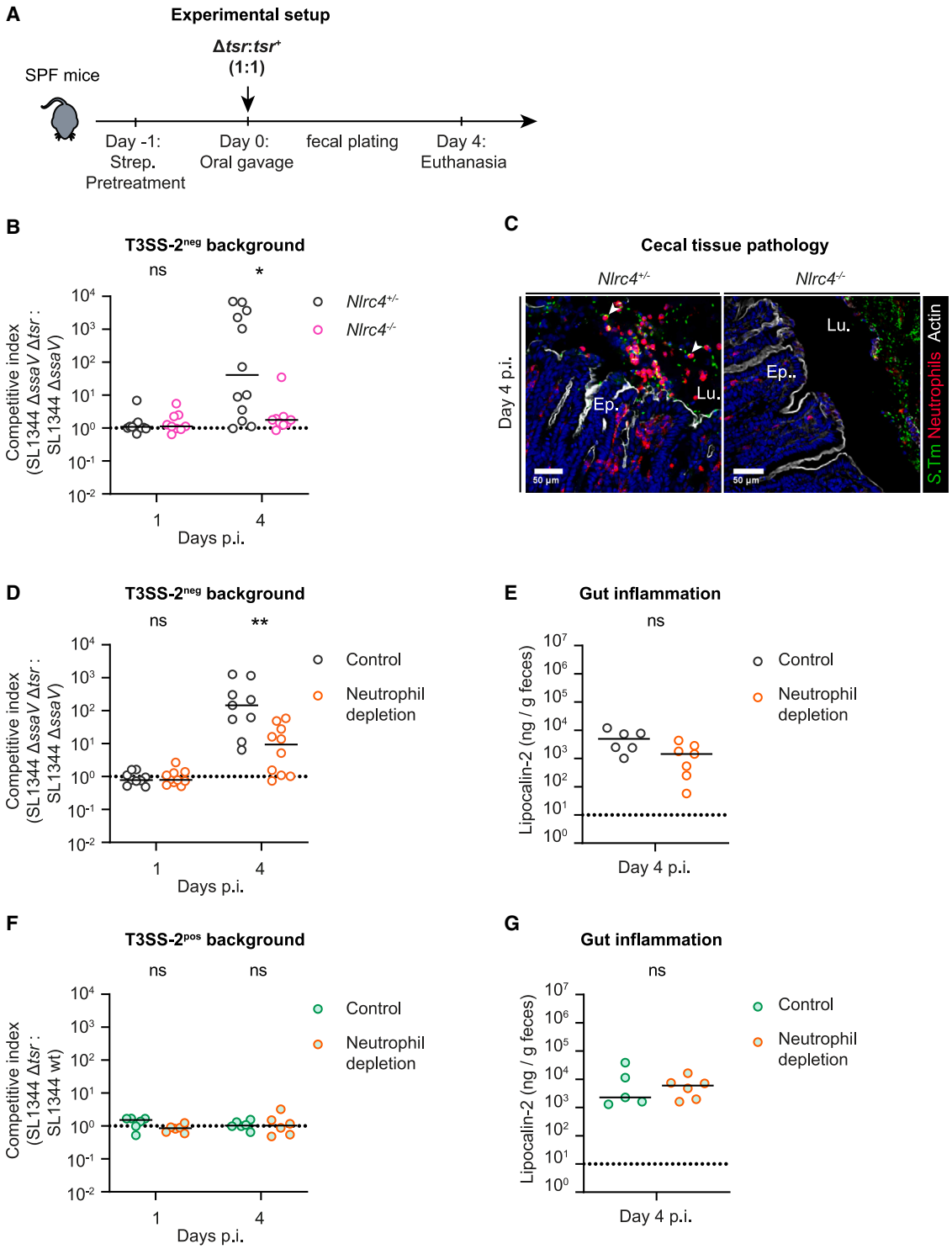

Figure 4. The role of Nlrc4 inflammasome and associated neutrophil recruitment in fitness disadvantage of *tsr*-proficient cells

(A) Experimental setup in (B)–(G).

(B and C) Competitive infections in streptomycin-pre-treated *Nlrc4*$^{+/-}$ (empty black circles) and *Nlrc4*$^{-/-}$ (empty pink circles) mice with SL1344 Δ*ssaV*Δ*tsr*:SL1344 Δ*ssaV* (1:1). (B) The C.I. in feces. (C) Representative micrographs of cecal tissue sections at day 4 p.i., stained for neutrophil marker Ly6B.2 and *Salmonella* LPS. Blue color: nuclei staining. Lu., lumen; Ep., epithelium. White arrows: *S.*Tm associated with neutrophils in the lumen. Scale bar: 50 μm.

(D–G) Competitive infections in streptomycin-pre-treated C56BL/6 mice with (D and E) SL1344 Δ*ssaV*Δ*tsr*:SL1344 Δ*ssaV* (1:1; control: empty black circles; neutrophil depleted: empty orange circles) and (F and G) SL1344 Δ*tsr*:SL1344 WT (1:1; control: green circles; re-plotted from Figure 1B, neutrophil depleted: filled

(legend continued on next page)

mutations we introduced did not influence the gut inflammation kinetics since the conditioning strain is 20-fold higher in abundance, which is sufficient to shape the inflammatory milieu in the gut.[5,51]

First, we tested if *tsr*-proficient cells have a fitness defect in the inflamed gut. Therefore, we compared the group 1 infection setup to the group 2 infection setup (see scheme in Figure 3A). To assess the induction of inflammation, we measured concentration of Lipocalin-2 (a broad marker for gut inflammation[42]) in the feces and analyzed the mRNA expression of pro-inflammatory cytokines and chemokines in the cecal tissue. The mice infected with the SL1344 Δ*ssaV*-conditioned strain mixture showed significantly higher fecal Lipoclain-2 levels than the mice infected without this conditioning strain (Figure 3B). Similarly, mRNA levels of cytokine and chemokines involved in immune responses to acute *Salmonella* infection were elevated in mice infected with the SL1344 Δ*ssaV*-conditioned mixture (Figure 3C). In addition, immunofluorescence microscopy analysis of infected cecal tissue sections revealed the typical signs[10,15] of enteropathy in mice infected with the SL1344 Δ*ssaV*, including expulsion of infected epithelial cells into the gut lumen and neutrophil infiltration (Figure 3D). Notably, in these mice, we observed that the pathogen cells were in close contact with the epithelium and with neutrophils in the gut lumen. In contrast, we observed neither epithelial cell expulsion nor neutrophil infiltration in mice infected only with the SL1344 Δ*invG* Δ*ssaV* (no conditioning; blue circles; Figures 3B and 3C), and the pathogen cells were mostly located in the gut lumen far away from the epithelium (Figure 3D). Strikingly, in the SL1344 Δ*ssaV*-conditioned gut, avirulent *S*.Tm *tsr* mutant cells outnumbered the Tsr-proficient avirulent *S*.Tm cells in feces at day 4 p.i. (Figures 3E and S3A; C.I. ≈100), while the *tsr*-deficient and -proficient populations remained at a 1:1 ratio in the feces of mice infected without the conditioning strain (Figures 3E and S3B, empty blue circles; C.I. ≈1). In fact, in the SL1344 Δ*ssaV*-conditioned gut, *tsr*-deficient cells reached the carrying capacity and caught up with the conditioning strain by day 4 p.i. (ca. 10^9 CFU/g feces; Figure S3A). Of further note, without the conditioning strain, total *Salmonella* loads were in general higher at day 1 p.i. and declined by day 4 p.i. (Figure S3B). This was likely attributable to the lack of gut inflammation, which favors microbiota regrowth that can exclude pathogen cells from the gut.[1] These data suggest that in the absence of functional T3SS-2, tsr^+ cells are attenuated compared to the *tsr* deletion mutant. This effect of T3SS-2 virulence appears to act globally on the total gut-luminal *S*.Tm population.

Second, we tested if the fitness defect of *tsr*-proficient cells during gut inflammation was indeed a chemotaxis-related phenomenon. Therefore, we compared the group 1 to the group 3 infection (see scheme in Figure 3A). In the latter group, *tsr*-deficient and -proficient cells of the SL1344 Δ*ssaV*Δ*cheY* background reached equal levels in the inflamed gut lumen, while *tsr*-proficient cells were outcompeted by the *tsr*-deficient cells when compared in the SL1344 Δ*invG*Δ*ssaV* background, as indicated by feces plating (Figures 3F and S3C; C.I. >100 vs. ≈1, respectively, at day 4 p.i.). Thus, we conclude that the fitness advantage of Δ*tsr* cells over tsr^+ cells in the SL1344 Δ*ssaV*-conditioned gut hinges on chemotaxis.

Taken together, these findings suggest that T3SS-2 virulence acts globally (in *trans*) to counteract the detrimental effects of host immune responses so that the pathogen can benefit from Tsr chemotaxis and efficiently exploit the inflamed gut.

NLRC4 inflammasome and luminal neutrophils impose the selection against *tsr*-proficient cells in the gut lumen

Next, we investigated which host factors contribute to the fitness loss of *tsr*-proficient cells. We and others previously showed that the early immune response to oral *Salmonella* infection in mice is mainly controlled by the epithelial NLRC4 inflammasome.[8,10] The recognition of the pathogen (and its virulence factors) by this defense system leads to a robust immune response in which infected epithelial cells are expelled[8,10,11,49] and luminal pathogen cells are decimated by neutrophils.[12,13] Therefore, we next tested if these immune responses might select against pathogen cells performing Tsr chemotaxis but lacking T3SS-2 virulence (Figure 4A). To test this hypothesis, we performed competitive infections in the SL1344 Δ*ssaV* background in Nlrc4 knockout (KO) ($Nlrc4^{-/-}$) mice and heterozygous littermate controls ($Nlrc4^{+/-}$). In control mice with a functional NLRC4 inflammasome, we observed a similar selection against *tsr*-proficient cells as in Figure 2, while this selection was dramatically reduced in $Nlrc4^{-/-}$ mice (day 4 p.i.; Figures 4B and S4A). Microscopy analysis of cecal tissue samples from $Nlrc4^{+/-}$ mice showed typical features of epithelial cell expulsion and neutrophil infiltration into the gut lumen at day 4 p.i. (Figure 4C), as we observed before in Figure 3D, and these intraluminal neutrophils seemed to form large aggregates around *S*.Tm cells. On the contrary, in $Nlrc4^{-/-}$ mice, we did not observe any such aggregates, and neutrophils and *S*.Tm cells were not in close contact (Figure 4C).

Activation of the NLRC4 inflammasome initiates a robust immune response characterized by the secretion of pro-inflammatory cytokines interleukin-1β (IL-1β) and IL-18 that results in massive immune cell influx into the gut lumen.[9] Neutrophils that are recruited by this response impose a strong bottleneck on the pathogen population in the gut lumen during acute *Salmonella* infection, and neutrophil depletion by an α-Ly6G antibody significantly reduces this effect.[12,13] Thus, we next tested if neutrophils select against pathogen cells performing Tsr chemotaxis and if T3SS-2 virulence can counteract this. For this purpose, we infected control and neutrophil-depleted mice with 1:1 mixtures of SL1344 Δ*ssaV*Δ*tsr* vs. SL1344 Δ*ssaV* or SL1344 Δ*tsr* vs. SL1344 WT and compared the C.I.s (*tsr* deficient/*tsr* proficient). In the SL1344 Δ*ssaV* background, *tsr*-proficient cells had a 100-fold fitness disadvantage compared to the *tsr*-deficient cells

orange circles). (D and F) The C.I. in feces. Dotted lines: C.I. of 1. (E and G) Fecal Lipocalin-2 concentrations (control data re-plotted from Figure 2C for each group). Dotted line: detection limit.

(B) 3 independent experiments for each group; $Nlrc4^{+/-}$ (n = 12 mice) and $Nlrc4^{-/-}$ (n = 9 mice). (D) 3 independent experiments for each group; control (n = 9 mice; 6 PBS control; 3 isotype control) and neutrophil depleted (n = 10 mice). (F) 2 independent experiments for each group; control (n = 6 mice; re-plotted from Figure 1B) and neutrophil depletion (n = 6 mice). Two-tailed Mann Whitney U tests to compare two groups. ns $p \geq 0.05$ and *$p < 0.05$.

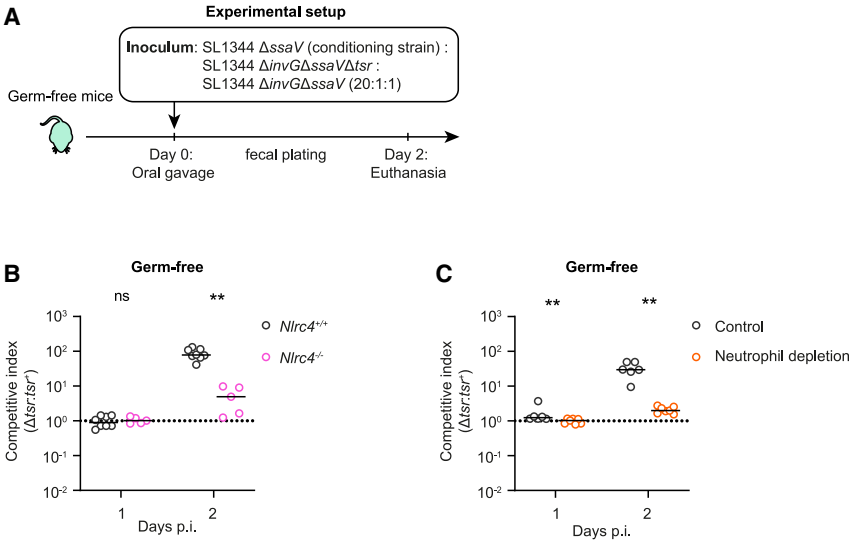

Figure 5. The role of gut microbiota in fitness disadvantage of *tsr*-proficient cells

(A) Experimental setup.

(B and C) Competitive infections in germ-free *Nlrc4*$^{+/+}$ (empty black circles) and *Nlrc4*$^{-/-}$ (empty pink circles) mice or in germ-free C57BL/6 mice (control: empty black circles; neutrophil depleted: empty orange circles) with SL1344 Δ*ssaV*:SL1344 Δ*invG*Δ*ssaV*Δ*tsr*:SL1344 Δ*invG*Δ*ssaV* (20:1:1). (B and C) The C.I. in feces. Lines: median. Dotted lines: C.I. of 1. (B) 2 independent experiments; 2 for *Nlrc4*$^{+/+}$ (n = 8 mice) and 1 for *Nlrc4*$^{-/-}$ (n = 5 mice). (C) 3 independent experiments for each group; control (n = 6 mice) and neutrophil depleted (n = 7 mice). Two-tailed Mann Whitney U tests to compare two groups. ns $p \geq 0.05$ and **$p < 0.01$.

by day 4 p.i. in control mice, while this disadvantage was essentially abolished in neutrophil-depleted mice (Figure 4D; C.I. ≈100 vs. ≈10 at day 4 p.i., respectively), despite the robust inflammation triggered also in these mice (Figure 4E). By contrast, in the SL1344 WT background, the C.I.s for *tsr*-proficient vs. *tsr*-deficient *S.*Tm were indistinguishable between the control mice and the neutrophil-depleted group (Figure 4F; C.I. ≈1 vs. ≈1 at day 4 p.i., respectively). Of note, a robust gut inflammation was again detectable also in neutrophil-depleted mice (Figure 4G). Thus, we conclude that immune responses controlled by the NLRC4 inflammasome and intraluminal neutrophils impose the detrimental effects of Tsr chemotaxis and that these detrimental effects are alleviated by T3SS-2 virulence.

Neutrophil-inflicted fitness loss of *tsr*-proficient cells is also observed in germ-free mice

Lastly, we investigated the role of the resident microbiota in shaping the selective landscape for Tsr-mediated chemotaxis. We and others have previously shown that the resident microbiota of the host can influence gut inflammation kinetics, the selection for certain mutants[35] and impact the type of metabolites secreted into the lumen during gut inflammation.[13,52–55] Therefore, we asked if the signal leading to Tsr-mediated chemotaxis of *Salmonella* cells in the gut lumen is host derived or if it might be produced or modulated by the microbiota. To test this, we performed competitive infection experiments (as in Figure 3A) in *Nlrc4*$^{-/-}$ and neutrophil-depleted germ-free mice. The inoculum consisted of SL1344 Δ*ssaV* (conditioning strain) and a pair of test strains (SL1344 Δ*invG*Δ*ssaV*Δ*tsr* and SL1344 Δ*invG*Δ*ssaV*; 20:1:1, respectively; Figure 5A; 2 day infection instead of 4 days, as germ-free mice are more susceptible to infection). First, we checked whether we could observe a fitness-defect associated with the Tsr chemotaxis in these mice. We found that the *tsr*-proficient test strain was attenuated in the feces compared to the *tsr*-deficient counterpart already by day 2 p.i. (Figure 5B; C.I. > 80). This suggests that Tsr-mediated chemotaxis and the associated fitness effects are occurring also in the absence of the gut microbiota. Second, we tested if the NLRC4 inflammasome was required for the observed fitness defect of the *tsr*-proficient strain. Similar to our results from Figure 4A, in germ-free *Nlrc4*$^{-/-}$ mice, the competitive disadvantage of *tsr*-proficient cells was greatly reduced in comparison to WT germ-free mice (Figures 5B and S5A, black circles vs. pink circles; median C.I.s of 78 vs. 7, respectively). Finally, we tested if neutrophils are critical for selecting against *tsr*-proficient *S.*Tm cells also in germ-free mice. To test this, we infected WT germ-free mice and depleted neutrophils as before. In the control mice, the pathogen cells carrying a functional Tsr receptor suffered from a ≈20-fold reduction in their fecal loads in comparison to the *tsr* mutant cells. In contrast, in the neutrophil-depleted mice, both *tsr*-proficient and -deficient populations grew almost equally well (Figures 5C and S5B, black circles vs. orange circles; C.I. ≈30 vs. ≈2.2, respectively). Therefore, these data indicate that the fitness defect associated with the Tsr-mediated chemotaxis in the absence of T3SS-2 is attributable to intraluminal neutrophils also in germ-free mice.

DISCUSSION

Previously, Tsr-dependent chemotaxis of *Salmonella* toward the epithelium was shown to be crucial for the pathogen to bloom in the inflamed gut,[6,7,31] while other studies reported that inflammation poses a significant danger to pathogen cells (particularly close to the epithelium).[12–14] This suggests the existence of a context-dependent fitness benefit for Tsr-mediated chemotaxis. Here, we present a systematic approach, which identified the host and the pathogen factors shaping the gut-luminal niche that selects for or against Tsr-mediated chemotaxis during acute *Salmonella* infection. Our findings imply that exploiting the energetically rich microhabitat (constructed around the gut epithelium) by *S.*Tm during gut inflammation is heavily dependent on subtle features of the intestinal immune response and the presence of additional virulence factors: namely, the T3SS-2 machinery, the T3SS-2 effectors, and, in particular, the effector protein SspH1, which is naturally encoded by the Gifsy3 prophage of

ATCC14028 (Figure 1). *S*.Tm strains like SL1344, which are missing one or more of these virulence factors, are not able to benefit from Tsr-mediated chemotaxis. More strikingly, in the absence of T3SS-2 machinery, the niche targeted via Tsr is in fact detrimental for the pathogen's fitness (i.e., SL1344 and ATCC14028 alike) in the inflamed gut, as the *tsr*-proficient cells cannot survive the neutrophil attack (Figures 2, 3, 4, and 5). These findings help to resolve apparently conflicting reports in the literature and provide a clear example of how interplay within the pathogen's virulence factor repertoire is decisive to reap a fitness benefit in the gut.

Our results reveal that the fitness advantage conferred by the Tsr chemotaxis receptor in the inflamed gut is intimately connected to carrying a functional T3SS-2. In the murine gut, *S*.Tm strains lacking this apparatus suffer from a severe fitness loss when engaging in Tsr chemotaxis. T3SS-2 of *S*.Tm is classically associated with intracellular growth and systemic spread and is therefore implicated in the formation of tissue reservoirs during long-term infection.[19–21] It is predicted that *S*.Tm has evolved as a pathogen through sequential acquisition of SPI-1 and SPI-2 via horizontal gene transfer from an *E. coli*-like ancestor.[56,57] While evolution of SPI-1-mediated virulence does make sense considering the direct fitness advantage conferred by gut inflammation,[1] the rationale for SPI-2-mediated virulence in terms of supporting colonization of the inflamed gut has not been well understood. Here, we suggest one mechanism by which T3SS-2 directly contributes to the fitness of the pathogen in the gut lumen during acute infection. Thus, these results extend our understanding of the evolution and the maintenance of SPI-2-encoded virulence. Strikingly, in our mouse infection experiments with 14028, Tsr only provided a fitness advantage in strains that harbored a prophage-encoded T3SS effector, SspH1. This suggests that beyond acquisition of central pathogenicity islands to generally promote fitness and survival from the immune response in the gut, accessory virulence factors may have later been acquired in strain-specific manners.[58–60] It is tempting to speculate that such modulatory effectors may define the strain's host range and allow adaptations to the precise makeup of local nutritional niches and the innate immune responses protecting the gut. Similarly, these findings may provide an explanation for why *tsr* mutations are selected in some natural situations.[36,37] Such selection for *tsr* mutations might, for example, occur in hosts that develop pronounced gut inflammation and that feature a configuration of the inflammasome-mediated mucosal defense, which cannot be efficiently controlled by the cocktail of T3SS effectors expressed by the infecting *Salmonella* strain. It is tempting to speculate that the stark variation in inflammasome-related genes of different hosts and their spectrum of sensitivity to different bacterial ligands might be a driving force that selects for ever-new *Salmonella* clones that have acquired new (and better matched) combinations of T3SS effectors to optimally control the antimicrobial effects of host gut inflammation. Thereby, horizontal transfer of new T3SS effectors might provide an important contribution to the adaptation of *Salmonella* spp. to their broad range of different hosts.

The exact mechanism by which T3SS-2 effectors interact with host immune defenses to turn Tsr-mediated chemotaxis toward a hostile environment into a fitness advantage remains to be fully investigated. Our data add to the evidence that the microhabitat constructed near the epithelium contains intraluminal neutrophils that can use a myriad of strategies to kill or immobilize extracellular pathogens (e.g., phagocytosis, release of reactive oxygen/nitrate species, and release of neutrophil extracellular traps.[61,62] Equipped with such an arsenal of defense mechanisms, neutrophils can transiently eliminate up to 99.9999% of the gut-luminal *S*.Tm population during acute gut infection, imposing a tight bottleneck.[12,13] Interestingly, a small portion of the *S*.Tm cells can survive this attack and grow back to very high population densities.[12,13] However, it remained unclear how *S*.Tm can re-bloom in the gut lumen after such a strong bottleneck. It is possible that SPI-2/T3SS-2-mediated virulence might provide a "survival shelter" during the neutrophil-mediated bottleneck. Notably, a previous report showed that *S*.Tm can indeed reside transiently inside luminal neutrophils.[63] Thus, it is plausible to speculate that "hiding inside the enemy" can be one way to avoid complete killing by neutrophils and that the surviving pathogen cells can then exploit the post-bottleneck gut lumen via Tsr-mediated chemotaxis. Alternatively, the effects mediated by T3SS-2 could contribute to conditioning the gut lumen. In theory, T3SS-2 may also promote survival within intestinal epithelial cells with subsequent pathogen re-entry into the gut lumen. However, our conditioning experiments in Figure 3 argue that the Tsr-dependent fitness is independent of the pathogen's capacity to invade or grow efficiently within host cells. Therefore, the T3SS-2-mediated conditioning of a gut-luminal niche appears more likely. This influence may occur on a global scale by modifying the quality or quantity of mucosal inflammation, or at fine spatial scales, such as through the manipulation of specific host cells. In this context, the modulation of the immune response by these effectors could prove advantageous for all luminal Enterobacteriaceae members. Previous reports have already illuminated mechanisms through which effectors, secreted via T3SS-2[64] or homologs in *Shigella flexneri*,[65,66] can interact with host inflammasome proteins such as NLRP3, NLRC4, or the pore-forming gasdermins, thereby subverting host immune responses. Furthermore, T3SS-2 effectors have the capacity to enhance the intracellular survival of *S*.Tm in epithelial cells, which was shown to enhance the luminal expansion and the chronic fecal shedding of the pathogen,[67] and the tissue infection may also affect the gut-luminal milieu. Additional research will be imperative to unravel the relevant host-manipulation mechanisms of T3SS-2 and the specific functions of its effectors in exploiting mucosal immune defenses.

A recent report highlighted the ability of commensal *E. coli* to invade the niche created by *Salmonella*-induced gut inflammation through Tsr-mediated chemotaxis.[7] In this report, *E. coli* cells were able to utilize the host-derived nitrate more efficiently than *Salmonella* and thereby reduce the pathogen's ability to colonize the gut. Of note, *S*.Tm ATCC14028 (14028) was used in that study, which carries the Gifsy3 prophage. Interestingly, in that study, commensal *E. coli* could exploit the same niche, constructed by the *Salmonella* virulence factors, using Tsr chemotaxis. This raises the question of how *E. coli* could benefit from this microhabitat despite detrimental effects of the gut

inflammation. It could thus be that the effect of *Salmonella* T3SS-2 on the host acts globally by modulating the relevant gut-luminal niche and thereby benefits neighboring cells that can perform chemotaxis toward the gut epithelium without being killed. This would further hint at the existence of mechanisms used by some bystander microbiota members to exploit gut inflammation. We propose that characterization of such mechanism(s) used by the resident microbiota to outcompete *Salmonella* under the pressure of gut inflammation might open the way to develop therapeutics to prevent gut colonization by enteric pathogens.

Many other enteric pathogens such as *C. rodentium*, *E. coli*, *V. cholerae*, and *C. difficile* trigger gut inflammation and exploit the energetically rich niche created upon host responses to the insult.[1–4,68] Studies so far have mainly explored the metabolic strategies used by these pathogens to gain specific advantages over other members of the gut microbiota during gut inflammation. However, as we showed in the present study on *Salmonella*, this environment can be deadly not only for the microbiota but also for the pathogen itself, unless it expresses specific ''enabling'' virulence factors (e.g., T3SS-2, SspH1). We propose that the described metabolic adaptations of other enteric pathogens might also prove to be coupled to such specific virulence features, and therefore further studies might reveal similar strategies.

Limitations of the study

It is important to note that most of the work (including ours) on the role of Tsr-mediated chemotaxis in the inflamed gut has been conducted in antibiotic-pre-treated mouse models. One pitfall of these models is that they bypass the initial ecosystem invasion. This speeds up pathogen growth in the gut lumen and accelerates and exacerbates the intensity of the immune response to acute *Salmonella* infection in these models. Therefore, the gut inflammation and its potentially detrimental effects on the microbiota and Tsr-dependent pathogen fitness may differ from most common natural infections, where a resident gut microbiota slows down the mucosal infection dynamics. To address this limitation, we recommend further evaluation of the role of Tsr and exploitation strategies in alternative model systems with milder microbiota perturbations, such as the recently established transient diet-shift model,[69] or alternative model systems that establish an inflammatory environment through methods like injection of lipopolysaccharide or other chemical substances.[69,70] Consequently, it is essential to recognize that our findings are specific to the strains and model systems described in this study. Further research will be necessary to determine the relevance of T3SS-2 and Tsr roles in other extant *Salmonella* strains.

Second, in this study, we focus on T3SS-2 apparatus mutants and an ATCC14028 mutant lacking *sspH1*. Therefore, we can only speculate about possible roles of other T3SS-2 effector proteins and if their expression might be modulated in *sspH1* or *ssaV* mutant strain backgrounds. A systematic analysis of the role of the different T3SS-2 effector proteins in controlling the benefits reaped by Tsr-dependent chemotaxis will be an interesting topic for future work.

Third, our conclusions from Figure 1 regarding the role of the 14028-specific prophage Gifsy3 and related effectors are based solely on the deletion of this section from the strain, demonstrating a correlation with the disappearance of the competitive advantage of the *tsr*$^+$ strain in the inflamed gut. However, our attempts to complement the entire region (prophage and the associated effectors) or to construct a complementation plasmid for *sspH1* have so far remained unsuccessful. Thus, we currently lack the evidence necessary to claim that this prophage and the T3SS effector(s) it harbors have a general effect on Tsr-related exploitation of gut inflammation. In particular, the absence of SspH1 in SL1344 raises questions about its role in counterselecting *tsr* in this strain background. While our study highlights the effect of deleting the genomic region from 14028, we acknowledge the need for additional experiments to ascertain whether the introduction of SspH1 into SL1344 rescues the counterselection of *tsr*. This proposed experiment would provide crucial insights into the specific role of SspH1 in the observed differences between SL1344 and 14028 strains. In light of these limitations, we emphasize the importance of further investigations to test the broader impact of Gifsy3 in promoting chemotaxis-related exploitation of gut inflammation across various *S*. Tm strains. Our study serves as a starting point, and we recommend future experiments to explore the generalizability of these findings.

Lastly, our assessment of gut inflammation relied mostly on measuring Lipocalin-2 concentration in fecal samples through ELISA in most of the figures. It is crucial to acknowledge that this protein can be secreted by both neutrophils and epithelial cells within the intestine. Therefore, while it serves as a valuable marker for broadly assessing the state of gut inflammation, also during intermittent time points of an ongoing infection, it alone may not be adequate to discern intricate changes in inflammation that might be most relevant for the selective features that promote or interfere with Tsr-dependent fitness.

STAR★METHODS

Detailed methods are provided in the online version of this paper and include the following:

- KEY RESOURCES TABLE
- RESOURCE AVAILABILITY
  - Lead contact
  - Materials availability
  - Data and code availability
- EXPERIMENTAL MODEL AND STUDY PARTICIPANT DETAILS
  - Bacterial strains and growth conditions
  - Mouse lines
- METHOD DETAILS
  - Construction of mutant bacterial strains
  - Mouse infection experiments
  - Immunofluorescence analysis
  - qRT-PCR
  - Lipocalin-2 ELISA
- QUANTIFICATION AND STATISTICAL ANALYSIS
  - Statistical analysis

SUPPLEMENTAL INFORMATION

Supplemental information can be found online at https://doi.org/10.1016/j.celrep.2024.113925.

ACKNOWLEDGMENTS

We would like to thank members of the Hardt lab, the Sunagawa lab, the Slack lab, and Médéric Diard for helpful discussions. We acknowledge the staff of the ETH Zürich mouse facility EPIC/RCHCI (especially Manuela Graf, Katharina Holzinger, Dennis Mollenhauer, Sven Nowok, and Dominik Bacovcin) and the staff of the Microbiology Institute. The Clean Mouse Facility is supported by the Genaxen Foundation, Inselspital, and the University of Bern. This work has been supported by grants from the Swiss National Science Foundation (310030_192567, NCCR Microbiomes) and the Monique Dornonville de la Cour Foundation to W.-D.H.

AUTHOR CONTRIBUTIONS

Conceptualization, E.G. and W.-D.H.; methodology, E.G., J.H., A.A.Y., L.M., and U.E.; investigation, E.G., J.H., A.A.Y., U.E., E.B., and W.-D.H.; technical assistance, U.E., J.Z., and M.E.S.; writing – original draft, E.G.; writing – review & editing, E.G., L.M., M.E.S., E.B., and W.-D.H.; visualization, E.G.; funding acquisition, W.-D.H.

DECLARATION OF INTERESTS

The authors declare no competing interests.

Received: June 23, 2023
Revised: January 12, 2024
Accepted: February 20, 2024

REFERENCES

1. Stecher, B., Robbiani, R., Walker, A.W., Westendorf, A.M., Barthel, M., Kremer, M., Chaffron, S., Macpherson, A.J., Buer, J., Parkhill, J., et al. (2007). Salmonella enterica Serovar Typhimurium Exploits Inflammation to Compete with the Intestinal Microbiota. PLoS Biol. *5*, 2177–2189. https://doi.org/10.1371/journal.pbio.0050244.
2. Lupp, C., Robertson, M.L., Wickham, M.E., Sekirov, I., Champion, O.L., Gaynor, E.C., and Finlay, B.B. (2007). Host-mediated inflammation disrupts the intestinal microbiota and promotes the overgrowth of Enterobacteriaceae. Cell Host & Microbe *2*. 204-129.
3. Rivera-Chávez, F., and Mekalanos, J.J. (2019). Cholera toxin promotes pathogen acquisition of host-derived nutrients. Nature *572*, 244–248. https://doi.org/10.1038/s41586-019-1453-3.
4. Pruss, K.M., and Sonnenburg, J.L. (2021). C. difficile exploits a host metabolite produced during toxin-mediated disease. Nature *593*, 261–265. https://doi.org/10.1038/s41586-021-03502-6.
5. Stecher, B., Barthel, M., Schlumberger, M.C., Haberli, L., Rabsch, W., Kremer, M., and Hardt, W.-D. (2008). Motility allows S. Typhimurium to benefit from the mucosal defence. Cell. Microbiol. *10*, 1166–1180. https://doi.org/10.1111/j.1462-5822.2008.01118.x.
6. Rivera-Chávez, F., Winter, S.E., Lopez, C.A., Xavier, M.N., Winter, M.G., Nuccio, S.-P., Russell, J.M., Laughlin, R.C., Lawhon, S.D., Sterzenbach, T., et al. (2013). Salmonella Uses Energy Taxis to Benefit from Intestinal Inflammation. PLoS Pathog. *9*, e1003267. https://doi.org/10.1371/journal.ppat.1003267.
7. Liou, M.J., Miller, B.M., Litvak, Y., Nguyen, H., Natwick, D.E., Savage, H.P., Rixon, J.A., Mahan, S.P., Hiyoshi, H., Rogers, A.W.L., et al. (2022). Host cells subdivide nutrient niches into discrete biogeographical microhabitats for gut microbes. Cell Host Microbe *30*, 836–847.e6. https://doi.org/10.1016/j.chom.2022.04.012.
8. Rauch, I., Deets, K.A., Ji, D.X., von Moltke, J., Tenthorey, J.L., Lee, A.Y., Philip, N.H., Ayres, J.S., Brodsky, I.E., Gronert, K., and Vance, R.E. (2017). NAIP-NLRC4 Inflammasomes Coordinate Intestinal Epithelial Cell Expulsion with Eicosanoid and IL-18 Release via Activation of Caspase-1 and -8. Immunity *46*, 649–659. https://doi.org/10.1016/j.immuni.2017.03.016.
9. Müller, A.A., Dolowschiak, T., Sellin, M.E., Felmy, B., Verbree, C., Gadient, S., Westermann, A.J., Vogel, J., LeibundGut-Landmann, S., and Hardt, W.-D. (2016). An NK Cell Perforin Response Elicited via IL-18 Controls Mucosal Inflammation Kinetics during Salmonella Gut Infection. PLoS Pathog. *12*, e1005723. https://doi.org/10.1371/journal.ppat.1005723.
10. Sellin, M.E., Müller, A.A., Felmy, B., Dolowschiak, T., Diard, M., Tardivel, A., Maslowski, K.M., and Hardt, W.-D. (2014). Epithelium-Intrinsic NAIP/NLRC4 Inflammasome Drives Infected Enterocyte Expulsion to Restrict Salmonella Replication in the Intestinal Mucosa. Cell Host Microbe *16*, 237–248. https://doi.org/10.1016/j.chom.2014.07.001.
11. Fattinger, S.A., Geiser, P., Samperio Ventayol, P., Di Martino, M.L., Furter, M., Felmy, B., Bakkeren, E., Hausmann, A., Barthel-Scherrer, M., Gül, E., et al. (2021). Epithelium-autonomous NAIP/NLRC4 prevents TNF-driven inflammatory destruction of the gut epithelial barrier in Salmonella-infected mice. Mucosal Immunol. *14*, 615–629. https://doi.org/10.1038/s41385-021-00381-y.
12. Maier, L., Diard, M., Sellin, M.E., Chouffane, E.-S., Trautwein-Weidner, K., Periaswamy, B., Slack, E., Dolowschiak, T., Stecher, B., Loverdo, C., et al. (2014). Granulocytes impose a tight bottleneck upon the gut luminal pathogen population during Salmonella typhimurium colitis. PLoS Pathog. *10*, e1004557.
13. Gül, E., Enz, U., Maurer, L., Abi Younes, A., Fattinger, S.A., Nguyen, B.D., Hausmann, A., Furter, M., Barthel, M., Sellin, M.E., and Hardt, W.-D. (2023). Intraluminal neutrophils limit epithelium damage by reducing pathogen assault on intestinal epithelial cells during Salmonella gut infection. PLoS Pathog. *19*, e1011235. https://doi.org/10.1371/journal.ppat.1011235.
14. Ackermann, M., Stecher, B., Freed, N.E., Songhet, P., Hardt, W.-D., and Doebeli, M. (2008). Self-destructive cooperation mediated by phenotypic noise. Nature *454*, 987–990. https://doi.org/10.1038/nature07067.
15. Hapfelmeier, S., Stecher, B., Barthel, M., Kremer, M., Müller, A.J., Heikenwalder, M., Stallmach, T., Hensel, M., Pfeffer, K., Akira, S., and Hardt, W.D. (2005). The Salmonella pathogenicity island (SPI)-2 and SPI-1 type III secretion systems allow Salmonella serovar typhimurium to trigger colitis via MyD88-dependent and MyD88-independent mechanisms. J. Immunol. *174*, 1675–1685.
16. Schlumberger, M.C., and Hardt, W.-D. (2006). Salmonella type III secretion effectors: pulling the host cell's strings. Curr. Opin. Microbiol. *9*, 46–54. https://doi.org/10.1016/j.mib.2005.12.006.
17. Fattinger, S.A., Sellin, M.E., and Hardt, W.-D. (2021). Salmonella effector driven invasion of the gut epithelium: breaking in and setting the house on fire. Curr. Opin. Microbiol. *64*, 9–18. https://doi.org/10.1016/j.mib.2021.08.007.
18. Jennings, E., Thurston, T.L.M., and Holden, D.W. (2017). Salmonella SPI-2 Type III Secretion System Effectors: Molecular Mechanisms And Physiological Consequences. Cell Host Microbe *22*, 217–231. https://doi.org/10.1016/j.chom.2017.07.009.
19. Helaine, S., Cheverton, A.M., Watson, K.G., Faure, L.M., Matthews, S.A., and Holden, D.W. (2014). Internalization of Salmonella by macrophages induces formation of nonreplicating persisters. Science *343*, 204–208.
20. Stapels, D.A.C., Hill, P.W.S., Westermann, A.J., Fisher, R.A., Thurston, T.L., Saliba, A.-E., Blommestein, I., Vogel, J., and Helaine, S. (2018). Salmonella persisters undermine host immune defenses during antibiotic treatment. Science *362*, 1156–1160. https://doi.org/10.1126/science.aat7148.
21. Pham, T.H.M., Brewer, S.M., Thurston, T., Massis, L.M., Honeycutt, J., Lugo, K., Jacobson, A.R., Vilches-Moure, J.G., Hamblin, M., Helaine, S., and Monack, D.M. (2020). Salmonella-Driven Polarization of Granuloma

Macrophages Antagonizes TNF-Mediated Pathogen Restriction during Persistent Infection. Cell Host Microbe *27*, 54–67.e5. https://doi.org/10.1016/j.chom.2019.11.011.

22. Bakkeren, E., Huisman, J.S., Fattinger, S.A., Hausmann, A., Furter, M., Egli, A., Slack, E., Sellin, M.E., Bonhoeffer, S., Regoes, R.R., et al. (2019). Salmonella persisters promote the spread of antibiotic resistance plasmids in the gut. Nature *573*, 276–280. https://doi.org/10.1038/s41586-019-1521-8.
23. Clark, L., Perrett, C.A., Malt, L., Harward, C., Humphrey, S., Jepson, K.A., Martinez-Argudo, I., Carney, L.J., La Ragione, R.M., Humphrey, T.J., and Jepson, M.A. (2011). Differences in Salmonella enterica serovar Typhimurium strain invasiveness are associated with heterogeneity in SPI-1 gene expression. Microbiology (Read.) *157*, 2072–2083. https://doi.org/10.1099/mic.0.048496-0.
24. Brüssow, H., Canchaya, C., and Hardt, W.-D. (2004). Phages and the evolution of bacterial pathogens: from genomic rearrangements to lysogenic conversion. Microbiol. Mol. Biol. Rev. *68*, 560–602.
25. Boyd, E.F. (2012). Chapter 4 - Bacteriophage-Encoded Bacterial Virulence Factors and Phage–Pathogenicity Island Interactions. In Advances in Virus Research, M. Łobocka and W.T. Szybalski, eds. (Academic Press), pp. 91–118. https://doi.org/10.1016/B978-0-12-394621-8.00014-5.
26. Tsolis, R.M., Townsend, S.M., Miao, E.A., Miller, S.I., Ficht, T.A., Adams, L.G., and Bäumler, A.J. (1999). Identification of a Putative *Salmonella enterica* Serotype Typhimurium Host Range Factor with Homology to IpaH and YopM by Signature-Tagged Mutagenesis. Infect. Immun. *67*, 6385–6393. https://doi.org/10.1128/IAI.67.12.6385-6393.1999.
27. Figueroa-Bossi, N., Uzzau, S., Maloriol, D., and Bossi, L. (2001). Variable assortment of prophages provides a transferable repertoire of pathogenic determinants in Salmonella. Mol. Microbiol. *39*, 260–271.
28. Miao, E.A., Scherer, C.A., Tsolis, R.M., Kingsley, R.A., Adams, L.G., Bäumler, A.J., and Miller, S.I. (1999). Salmonella typhimurium leucine-rich repeat proteins are targeted to the SPI1 and SPI2 type III secretion systems. Mol. Microbiol. *34*, 850–864. https://doi.org/10.1046/j.1365-2958.1999.01651.x.
29. Bullones-Bolaños, A., Bernal-Bayard, J., and Ramos-Morales, F. (2022). The NEL Family of Bacterial E3 Ubiquitin Ligases. Int. J. Mol. Sci. *23*, 7725.
30. Cook, M., Delbecq, S.P., Schweppe, T.P., Guttman, M., Klevit, R.E., and Brzovic, P.S. (2019). The ubiquitin ligase SspH1 from Salmonella uses a modular and dynamic E3 domain to catalyze substrate ubiquitylation. J. Biol. Chem. *294*, 783–793.
31. Rivera-Chávez, F., Lopez, C.A., Zhang, L.F., García-Pastor, L., Chávez-Arroyo, A., Lokken, K.L., Tsolis Renée, M., Winter, S.E., and Bäumler, A.J. (2016). Energy Taxis toward Host-Derived Nitrate Supports a Salmonella Pathogenicity Island 1-Independent Mechanism of Invasion. mBio *7*, e00960-16–e00916. https://doi.org/10.1128/mBio.00960-16.
32. Winter, S.E., Winter, M.G., Xavier, M.N., Thiennimitr, P., Poon, V., Keestra, A.M., Laughlin, R.C., Gomez, G., Wu, J., Lawhon, S.D., et al. (2013). Host-Derived Nitrate Boosts Growth of *E. coli* in the Inflamed Gut. Science *339*, 708–711. https://doi.org/10.1126/science.1232467.
33. Hansen, C.H., Endres, R.G., and Wingreen, N.S. (2008). Chemotaxis in Escherichia coli: a molecular model for robust precise adaptation. PLoS Comput. Biol. *4*, e1.
34. Diard, M., Garcia, V., Maier, L., Remus-Emsermann, M.N.P., Regoes, R.R., Ackermann, M., and Hardt, W.-D. (2013). Stabilization of cooperative virulence by the expression of an avirulent phenotype. Nature *494*, 353–356.
35. Gül, E., Bakkeren, E., Salazar, G., Steiger, Y., Abi Younes, A., Clerc, M., Christen, P., Fattinger, S.A., Nguyen, B.D., Kiefer, P., et al. (2023). The microbiota conditions a gut milieu that selects for wild-type Salmonella Typhimurium virulence. PLoS Biol. *21*, e3002253. https://doi.org/10.1371/journal.pbio.3002253.
36. Bawn, M., Alikhan, N.-F., Thilliez, G., Kirkwood, M., Wheeler, N.E., Petrovska, L., Dallman, T.J., Adriaenssens, E.M., Hall, N., and Kingsley, R.A. (2020). Evolution of Salmonella enterica serotype Typhimurium driven by anthropogenic selection and niche adaptation. PLoS Genet. *16*, e1008850.
37. Cherry, J.L. (2020). Selection-driven gene inactivation in Salmonella. Genome Biol. Evol. *12*, 18–34.
38. Le Minor, L., and Popoff, M.Y. (1987). Request for an opinion: Designation of Salmonella enterica sp. nov., nom. rev., as the type and only species of the genus Salmonella. Int. J. Syst. Bacteriol. *37*, 465–468.
39. Rankin, J.D., and Taylor, R.J. (1966). The estimation of doses of Salmonella typhimurium suitable for the experimental production of disease in calves. Vet. Rec. *78*, 706–707. https://doi.org/10.1136/vr.78.21.706.
40. Hoiseth, S.K., and Stocker, B.A. (1981). Aromatic-dependent Salmonella typhimurium are non-virulent and effective as live vaccines. Nature *291*, 238–239.
41. Barthel, M., Hapfelmeier, S., Quintanilla-Martínez, L., Kremer, M., Rohde, M., Hogardt, M., Pfeffer, K., Rüssmann, H., and Hardt, W.-D. (2003). Pretreatment of mice with streptomycin provides a Salmonella enterica serovar Typhimurium colitis model that allows analysis of both pathogen and host. Infect. Immun. *71*, 2839–2858.
42. Moor, K., Diard, M., Sellin, M.E., Felmy, B., Wotzka, S.Y., Toska, A., Bakkeren, E., Arnoldini, M., Bansept, F., Co, A.D., et al. (2017). High-avidity IgA protects the intestine by enchaining growing bacteria. Nature *544*, 498–502. https://doi.org/10.1038/nature22058.
43. Kropinski, A.M., Sulakvelidze, A., Konczy, P., and Poppe, C. (2007). Salmonella Phages and Prophages—Genomics and Practical Aspects. Salmonella: Methods and Protocols, 133–175.
44. Hiley, L., Fang, N.-X., Micalizzi, G.R., and Bates, J. (2014). Distribution of Gifsy-3 and of variants of ST64B and Gifsy-1 prophages amongst Salmonella enterica Serovar Typhimurium isolates: evidence that combinations of prophages promote clonality. PLoS One *9*, e86203.
45. Avraham, R., Haseley, N., Brown, D., Penaranda, C., Jijon, H.B., Trombetta, J.J., Satija, R., Shalek, A.K., Xavier, R.J., Regev, A., and Hung, D.T. (2015). Pathogen Cell-to-Cell Variability Drives Heterogeneity in Host Immune Responses. Cell *162*, 1309–1321. https://doi.org/10.1016/j.cell.2015.08.027.
46. Keszei, A.F.A., Tang, X., McCormick, C., Zeqiraj, E., Rohde, J.R., Tyers, M., and Sicheri, F. (2014). Structure of an SspH1-PKN1 complex reveals the basis for host substrate recognition and mechanism of activation for a bacterial E3 ubiquitin ligase. Mol. Cell Biol. *34*, 362–373.
47. Haraga, A., and Miller, S.I. (2003). A Salmonella enterica serovar Typhimurium translocated leucine-rich repeat effector protein inhibits NF-κB-dependent gene expression. Infect. Immun. *71*, 4052–4058.
48. Stecher, B., Paesold, G., Barthel, M., Kremer, M., Jantsch, J., Stallmach, T., Heikenwalder, M., and Hardt, W.-D. (2006). Chronic *Salmonella enterica* Serovar Typhimurium-Induced Colitis and Cholangitis in Streptomycin-Pretreated *Nramp1*$^{+/+}$ Mice. Infect. Immun. *74*, 5047–5057. https://doi.org/10.1128/iai.00072-06.
49. Hausmann, A., Böck, D., Geiser, P., Berthold, D.L., Fattinger, S.A., Furter, M., Bouman, J.A., Barthel-Scherrer, M., Lang, C.M., Bakkeren, E., et al. (2020). Intestinal epithelial NAIP/NLRC4 restricts systemic dissemination of the adapted pathogen Salmonella Typhimurium due to site-specific bacterial PAMP expression. Mucosal Immunol. *13*, 530–544.
50. Fattinger, S.A., Maurer, L., Geiser, P., Bernard, E.M., Enz, U., Ganguillet, S., Gül, E., Kroon, S., Demarco, B., Mack, V., et al. (2023). Gasdermin D is the only Gasdermin that provides protection against acute *Salmonella* gut infection in mice. Proc. Natl. Acad. Sci. USA *120(48)*, e2315503120. https://doi.org/10.1073/pnas.2315503120.
51. Stecher, B., Hapfelmeier, S., Müller, C., Kremer, M., Stallmach, T., and Hardt, W.-D. (2004). Flagella and Chemotaxis Are Required for Efficient Induction of Salmonella enterica Serovar Typhimurium Colitis in Streptomycin-Pretreated Mice. Infect. Immun. *72*, 4138–4150. https://doi.org/10.1128/IAI.72.7.4138-4150.2004.

52. Stecher, B., Macpherson, A.J., Hapfelmeier, S., Kremer, M., Stallmach, T., and Hardt, W.-D. (2005). Comparison of Salmonellaenterica Serovar Typhimurium Colitis in Germfree Mice and Mice Pretreated with Streptomycin. Infect. Immun. *73*, 3228–3241. https://doi.org/10.1128/IAI.73.6.3228-3241.2005.

53. Byndloss, M.X., and Bäumler, A.J. (2018). The germ-organ theory of noncommunicable diseases. Nat. Rev. Microbiol. *16*, 103–110.

54. Hockenberry, A.M., Micali, G., Takács, G., Weng, J., Hardt, W.-D., and Ackermann, M. (2021). Microbiota-derived metabolites inhibit Salmonella virulent subpopulation development by acting on single-cell behaviors. Proc. Natl. Acad. Sci. USA *118*, e2103027118.

55. Gül, E., Abi Younes, A., Huuskonen, J., Diawara, C., Nguyen, B.D., Maurer, L., Bakkeren, E., and Hardt, W.-D. (2023). Differences in carbon metabolic capacity fuel co-existence and plasmid transfer between Salmonella strains in the mouse gut. Cell Host Microbe *31*, 1140–1153.e3. https://doi.org/10.1016/j.chom.2023.05.029.

56. Desai, P.T., Porwollik, S., Long, F., Cheng, P., Wollam, A., Bhonagiri-Palsikar, V., Hallsworth-Pepin, K., Clifton, S.W., Weinstock, G.M., and McClelland, M. (2013). Evolutionary Genomics of Salmonella enterica Subspecies. mBio *4*, e00579-12–e00512. https://doi.org/10.1128/mBio.00579-12.

57. Diard, M., and Hardt, W.-D. (2017). Evolution of bacterial virulence. FEMS Microbiol. Rev. *41*, 679–697.

58. Langridge, G.C., Fookes, M., Connor, T.R., Feltwell, T., Feasey, N., Parsons, B.N., Seth-Smith, H.M.B., Barquist, L., Stedman, A., Humphrey, T., et al. (2015). Patterns of genome evolution that have accompanied host adaptation in Salmonella. Proc. Natl. Acad. Sci. USA *112*, 863–868.

59. Mirold, S., Rabsch, W., Rohde, M., Stender, S., Tschäpe, H., Rüssmann, H., Igwe, E., and Hardt, W.-D. (1999). Isolation of a temperate bacteriophage encoding the type III effector protein SopE from an epidemic Salmonella typhimurium strain. Proc. Natl. Acad. Sci. USA *96*, 9845–9850. https://doi.org/10.1073/pnas.96.17.9845.

60. Bäumler, A.J., Tsolis, R.M., Ficht, T.A., and Adams, L.G. (1998). Evolution of Host Adaptation in Salmonella enterica. Infect. Immun. *66*, 4579–4587. https://doi.org/10.1128/iai.66.10.4579-4587.1998.

61. Rosales, C. (2018). Neutrophil: A Cell with Many Roles in Inflammation or Several Cell Types? Front. Physiol. *9*, 113. https://doi.org/10.3389/fphys.2018.00113.

62. Fournier, B.M., and Parkos, C.A. (2012). The role of neutrophils during intestinal inflammation. Mucosal Immunol. *5*, 354–366. https://doi.org/10.1038/mi.2012.24.

63. Loetscher, Y., Wieser, A., Lengefeld, J., Kaiser, P., Schubert, S., Heikenwalder, M., Hardt, W.-D., and Stecher, B. (2012). Salmonella transiently reside in luminal neutrophils in the inflamed gut. PLoS One *7*, e34812.

64. Bierschenk, D., Monteleone, M., Moghaddas, F., Baker, P.J., Masters, S.L., Boucher, D., and Schroder, K. (2019). The Salmonella pathogenicity island-2 subverts human NLRP3 and NLRC4 inflammasome responses. J. Leukoc. Biol. *105*, 401–410.

65. Zhong, X., Zeng, H., Zhou, Z., Su, Y., Cheng, H., Hou, Y., She, Y., Feng, N., Wang, J., Shao, F., and Ding, J. (2023). Structural mechanisms for regulation of GSDMB pore-forming activity. Nature *616*, 598–605. https://doi.org/10.1038/s41586-023-05872-5.

66. Luchetti, G., Roncaioli, J.L., Chavez, R.A., Schubert, A.F., Kofoed, E.M., Reja, R., Cheung, T.K., Liang, Y., Webster, J.D., Lehoux, I., et al. (2021). Shigella ubiquitin ligase IpaH7.8 targets gasdermin D for degradation to prevent pyroptosis and enable infection. Cell Host Microbe *29*, 1521–1530.e10. https://doi.org/10.1016/j.chom.2021.08.010.

67. Chong, A., Cooper, K.G., Kari, L., Nilsson, O.R., Hillman, C., Fleming, B.A., Wang, Q., Nair, V., and Steele-Mortimer, O. (2021). Cytosolic replication in epithelial cells fuels intestinal expansion and chronic fecal shedding of Salmonella Typhimurium. Cell Host Microbe *29*, 1177–1185.e6. https://doi.org/10.1016/j.chom.2021.04.017.

68. Bäumler, A.J., and Sperandio, V. (2016). Interactions between the microbiota and pathogenic bacteria in the gut. Nature *535*, 85–93. https://doi.org/10.1038/nature18849.

69. Wotzka, S.Y., Kreuzer, M., Maier, L., Arnoldini, M., Nguyen, B.D., Brachmann, A.O., Berthold, D.L., Zünd, M., Hausmann, A., Bakkeren, E., et al. (2019). Escherichia coli limits Salmonella Typhimurium infections after diet shifts and fat-mediated microbiota perturbation in mice. Nat. Microbiol. *4*, 2164–2174. https://doi.org/10.1038/s41564-019-0568-5.

70. Hausmann, A., Felmy, B., Kunz, L., Kroon, S., Berthold, D.L., Ganz, G., Sandu, I., Nakamura, T., Zangger, N.S., Zhang, Y., et al. (2021). Intercrypt sentinel macrophages tune antibacterial NF-κB responses in gut epithelial cells via TNF. J. Exp. Med. *218*, e20210862. https://doi.org/10.1084/jem.20210862.

71. Jarvik, T., Smillie, C., Groisman, E.A., and Ochman, H. (2010). Short-term signatures of evolutionary change in the Salmonella enterica serovar Typhimurium 14028 genome. J. Bacteriol. *192*, 560–567.

72. Datsenko, K.A., and Wanner, B.L. (2000). One-step inactivation of chromosomal genes in Escherichia coli K-12 using PCR products. Proc. Natl. Acad. Sci. USA *97*, 6640–6645. https://doi.org/10.1073/pnas.120163297.

73. Sternberg, N.L., and Maurer, R. (1991). [2] Bacteriophage-mediated generalized transduction in Escherichia coli and Salmonella typhimurium. In Methods in Enzymology (Academic Press), pp. 18–43. https://doi.org/10.1016/0076-6879(91)04004-8.

74. Mariathasan, S., Newton, K., Monack, D.M., Vucic, D., French, D.M., Lee, W.P., Roose-Girma, M., Erickson, S., and Dixit, V.M. (2004). Differential activation of the inflammasome by caspase-1 adaptors ASC and Ipaf. Nature *430*, 213–218.

75. Kröger, C., Dillon, S.C., Cameron, A.D.S., Papenfort, K., Sivasankaran, S.K., Hokamp, K., Chao, Y., Sittka, A., Hébrard, M., Händler, K., et al. (2012). The transcriptional landscape and small RNAs of Salmonella enterica serovar Typhimurium. Proc. Natl. Acad. Sci. USA *109*, E1277–E1286. https://doi.org/10.1073/pnas.1201061109.

76. Stecher, B., Denzler, R., Maier, L., Bernet, F., Sanders, M.J., Pickard, D.J., Barthel, M., Westendorf, A.M., Krogfelt, K.A., Walker, A.W., et al. (2012). Gut inflammation can boost horizontal gene transfer between pathogenic and commensal Enterobacteriaceae. Proc. Natl. Acad. Sci. USA *109*, 1269–1274. https://doi.org/10.1073/pnas.1113246109.

STAR★METHODS

KEY RESOURCES TABLE

REAGENT or RESOURCE	SOURCE	IDENTIFIER
Antibodies		
α-S.Tm LPS	Difco	RRID: AB_2884995
α-mouse-Ly6B.2 (7/4)	BioRad	Cat# MCA771G; AB_322950
α-rabbit-AlexaFluor488	Abcam Biochemicals	RRID: AB_2630356
α-rat-Cy3	Jackson	RRID:AB_2338251
AlexaFluor647-conjugated Phalloidin	Santa Cruz Biotechnology	Cat# sc-363797
α-mouse-Ly6G (1A8)	BioXcell	Cat# BE0075-1; RRID: AB_1107721
Bacterial and virus strains		
Bacterial strains	see Table S1	N/A
Critical commercial assays		
Phusion™ Plus DNA Polymerase	ThermoFisher Scientific	F630L
QIAquick PCR Purification Kit	Qiagen	28104
Mouse Lipocalin-2/NGAL DuoSet ELISA	R&D Systems	DY1857
Deposited data		
Raw data used in the manuscript	This manuscript	doi.org/10.3929/ethz-b-000661105
Experimental models: Organisms/strains		
Mouse: 129SvEv SPF	Max von Pettenkofer-Institute, Munich, Germany	N/A
Mouse: C57BL/6 SPF	Jackson Laboratories; bred at EPIC mouse facility of ETH Zurich, Switzerland	RRID:IMSRJAX:000664
Mouse: C57BL/6 Germ-free	Jackson Laboratories; bred at EPIC mouse facility of ETH Zurich, Switzerland	C57BL/6J GF
Mouse: NLRC4 KO C57BL/6 Germ-free	Clean Mouse Facility of University of Bern, Bern, Switzerland	N/A
Oligonucleotides		
For stain preparation	See Table S2	N/A
For qPCR	See Table S4	N/A
Recombinant DNA		
Plasmids	See Table S3	N/A
Software and algorithms		
Graphpad Prism Version 9.0 for Windows	GraphPad Software, La Jolla California USA	Home - GraphPad

RESOURCE AVAILABILITY

Lead contact

Further information and requests for resources and reagents should be directed to and will be fulfilled by the lead contact, Wolf-Dietrich Hardt (hardt@micro.biol.ethz.ch).

Materials availability

Mouse lines used in this study can be obtained from Jackson laboratories. Gnotobiotic and genetically modified mice are available upon request. Newly generated bacterial strains are available upon request. All unique/stable reagents generated in this study are available from the lead contact with a completed materials transfer agreement.

Data and code availability

- All data reported in this paper will be shared by the lead contact upon request and deposited as raw data in the ETH Research Collection (an open-access source) with the following accession number: https://doi.org/10.3929/ethz-b-000661105
- This paper does not report original code.
- Any additional information required to reanalyze the data reported in this paper is available from the lead contact upon request.

EXPERIMENTAL MODEL AND STUDY PARTICIPANT DETAILS

Bacterial strains and growth conditions

In all experiments, *Salmonella* Typhimurium *S*.Tm SL1344[40] or *S*.Tm ATCC14028,[71] along with specified mutant variations (as outlined in key resources table), were utilized. The creation of gene deletion mutants or the incorporation of antibiotic resistance markers involved employing the λ red system, following the methodology detailed in Datsenko and Wanner.[72] Briefly, an antibiotic resistance cassette was introduced to replace the gene of interest using primers with approximately 40bp of the gene flanking regions and 20bp of the desired antibiotic resistance cassette (key resources table). The details of the protocol are explained in the Method Details. To address potential mutations caused by lambda-red induction and mutant preparation, P-22[73] lysates were made of the original mutant strains and used to subsequently transduce the mutation into the ancestral strain. The resultant genetic constructs were then transferred into the corresponding host strains via P22 HT105/1 int-201 phage transduction.[73] If necessary, antibiotic resistance modules were eliminated using the pCP20-encoded heat-inducible FLP recombinase.[72] For mouse infection experiments, bacteria were cultured in lysogeny broth (LB) supplemented with appropriate antibiotics antibiotics (50 μg/mL streptomycin (AppliChem); 15 μg/mL chloramphenicol (AppliChem); 50 μg/mL kanamycin (AppliChem); 100 μg/mL ampicillin (AppliChem)) at 37°C for 12 h and sub-cultured in a 1:20 LB dilution without antibiotics for 4 h. The cells were subsequently washed and suspended in cold PBS (BioConcept).

Mouse lines

The experiments were conducted using 8–12-week-old male or female mice. The sample size was not predetermined, and the mice were randomly allocated to different groups. Wild type mice were descendants of C57BL/6 (breeders originally obtained from Jackson laboratories) or 129SvEv(breeders originally obtained from Max von Pettenkofer-Institute, Munich, Germany), which have a standard complex microbiota (specific pathogen-free; SPF) and bred in controlled environments within individually ventilated cages at the EPIC and RCHCI mouse facilities of ETH Zurich in Switzerland. Germ-free C57BL/6 mice were raised in flexible film isolators, ensuring stringent measures to prevent microbial contamination at the EPIC mouse facility of ETH Zurich. Besides, the following genetically modified mouse lines were used: *Nlrc4*$^{-/-}$ (B6.C2-Nlrc4tm1Vmd,[74] *Nlrc4*$^{-/-}$ GF). *Nlrc4*$^{-/-}$ GF mice were derived germ free in the Clean Mouse Facility of University of Bern and kept in flexible film isolators at the ETH Zürich mouse facility upon transfer.

All studies were performed in accordance with ethical and legal requirements and were reviewed and approved by the Kantonales Veterinäramt Zürich under the licenses ZH193/2016, ZH158/2019, ZH108/2022, and ZH109/2022.[75,76]

METHOD DETAILS

Construction of mutant bacterial strains

Fresh gene knockout strains were generated utilizing the lambda-red single-step protocol.[72] In this approach, the gene of interest is replaced with an antibiotic resistance cassette. Initially, primers with approximately 40 base pairs representing the gene's flanking regions and an additional 20 base pairs for the desired antibiotic resistance cassette were developed (as listed in the Key Resources Table). Subsequently, DNA constructs were created using plasmids pKD3 and pKD4 for chloramphenicol and kanamycin, respectively, to implement the antibiotic resistance cassette flanked by the gene's regions. These constructs were generated using Phusion high-fidelity DNA polymerase, and the resulting PCR product was purified using the Qiagen DNA purification kit. For the preparation of highly concentrated competent cells, a strain containing the pKD46 plasmid, carrying the lambda-red phage and an ampicillin resistance cassette, was cultivated for 3 h at 30°C in 50mL LB-ampicillin supplemented with 10mM Arabinose (Sigma-Aldrich). This induced the phage-derived genes encoded on pKD46, with the plasmid being lost at 37°C. The cells were washed, concentrated via a series of centrifugation and resuspension steps in ice-cold H_2O, and then transformed with 5μL of the purified PCR product through electroporation at 1.8kV for 5ms. Following this, the cells were allowed to recover in warm LB for 1.5 h at 37°C and were then plated on LB plates containing the corresponding antibiotic to identify colonies featuring the desired gene knockout. Due to the potential risk of lambda-red induction and mutant preparation causing mutations elsewhere in the genome, P-22 lysates were generated from the original mutant strains and subsequently utilized to transfer the mutation into the ancestral strain.

Mouse infection experiments

Mice were pretreated with single dose of ampicillin (20 mg/mouse) or streptomycin (25 mg/mouse) 1 day before the infection and infected by oral gavage on the day 0 with the relevant S.Tm strain(s) as described in each figure. Germ-free mice infections were done similarly but without any antibiotic pretreatment.

For all infection experiments, the inocula were prepared as outlined. Overnight cultures of *S*.Tm in LB with streptomycin were subcultured for 4 h (1:20 dilution) in LB without antibiotics. Subsequently, the strains were washed with PBS, and mice received an oral gavage of approximately 5×10^7 CFU *S*.Tm. In competitive infection experiments, respective strains were separately prepared (subcultured and washed) and combined before oral gavage, based on the specified ratios in the figure legends. Feces were collected in pre-weighed tubes with 1mL PBS and homogenized with a steel ball for 2 min at 25 Hz. Daily monitoring of infected mice for their health status was conducted as described in the relevant license. Organs were harvested at the designated time points in each figure. For cecal tissue plating, the gentamicin protection assay was utilized to clear extracellular bacteria. The cecal tissue was

longitudinally cut, rapidly washed in PBS (3x), incubated for 45–75 min in PBS/400 μg/ml gentamicin (Sigma-Aldrich) at room temperature, and extensively washed (3 × 30s) in PBS before plating. The samples were homogenized using a tissue lyser (Qiagen) for 2 min at 25Hz frequency (cecal tissue for 3 min at 30Hz). These homogenized samples were diluted in PBS, plated on MacConkey (Oxoid) plates supplemented with the relevant antibiotic(s), and incubated at 37°C overnight. The following day, colonies were counted and represented as CFU/g content. The competitive index (C.I.) was calculated as the ratio of the mutant over wild type in the feces or organs, normalized to the initial ratio in the inoculum.

For *in vivo* depletion of neutrophils, anti-Ly6G (BioXCell, 1A8) was injected intraperitoneally at each day starting at a day before the start of the infection (250 μg/mouse).

Immunofluorescence analysis

Cecal tissue sections obtained from euthanized mice were fixed in 4% paraformaldehyde for 4 h at room temperature before being submerged in 20% sucrose/PBS solution, embedded in Optimal Cutting Temperature compound (OCT, Tissue-Tek), and snap-frozen using a liquid nitrogen solution. The samples were then stored at −80°C until further analysis. Following this, 10 μm cross-sections were prepared and mounted on glass slides (Superfrost++, Thermo Scientific). The slides containing the cryosections were air-dried at RT for a minimum of 12 h, rehydrated with PBS, and permeabilized using a 0.5% Triton X-100/PBS solution. For blocking, to ensure effective staining, the sections were initially treated with a 10% Normal Goat Serum (NGS)/PBS solution before applying primary and secondary antibodies. The antibodies used for staining included α-*S*.Tm LPS (O-antigen group B factor 4–5, Difco) at a 1:200 dilution, or α-Ly6B.2 clone 7/4 (BioRad) also at 1:200, in combination with suitable secondary antibodies (α-rabbit-AlexaFluor488 from Abcam Biochemicals, α-rat-Cy3 from Jackson) and fluorescent probes, such as CruzFluor488-conjugated Phalloidin (Santa Cruz Biotechnology), AlexaFluor647-conjugated Phalloidin (Molecular Probes), and/or DAPI (Sigma Aldrich). Once stained, the sections were covered with a glass slip using Mowiol (VWR International AG) and kept in the dark at RT overnight. For imaging, a Zeiss Axiovert 200m microscope equipped with 10-100x objectives or a spinning disc confocal lased unit (Visitron) with similar objectives were utilized. The obtained images were processed and analyzed using Visiview (Visitron) and/or ImageJ.

qRT-PCR

Cecal tissue samples from infected or control animals were gathered and snap-frozen in RNAlater solution (Thermo Fisher Scientific) after thorough PBS washing to eliminate the luminal content. The samples were preserved at −80°C until subjected to qRT-PCR analysis. For this, total RNA was extracted using the RNeasy Mini Kit (Qiagen) and then converted to cDNAs utilizing the RT2 HT First Strand cDNA Kit (Qiagen) following the manufacturer's protocol. Subsequently, qPCR was executed employing FastStart Universal SYBR Green Master reagents (Roche), and Ct values were captured using the QuantStudio 7 Flex FStepOne Plus Cycler. Primer design was facilitated by the NCBI primer-designing tool (Key Resources Table). The mRNA expression levels were depicted relative to the β-actin housekeeping gene ($2^{-\Delta Ct}$)), with specific comparisons outlined in the figure captions.

Lipocalin-2 ELISA

The Lipocalin-2 ELISA (R & D Systems) was conducted on fecal samples following the manufacturer's guidelines. Fecal pellets were suspended in PBS, with dilutions of 1:20, 1:400, or left undiluted, and concentrations were determined using Four-Parametric Logistic Regression curve fitting.

QUANTIFICATION AND STATISTICAL ANALYSIS

Statistical analysis

Where applicable, the two-tailed Mann Whitney-U test or Wilcoxon matched-pairs signed rank test was used to assess statistical significance as indicated in the figure legends. GraphPad Prism 9 for Windows was used for statistical testing. p values of $p \geq 0.05$ not significant (ns), $p < 0.05$ (*), $p < 0.01$ (**), $p < 0.001$ (***), and $p < 0.0001$ (****).